REGISTERED No M. 2121

OF MICHIGAN
JAN 16 1961

PROCEEDINGS

OF THE

INDIAN ACADEMY OF SCIENCES

VOL. LII] SECTION A [No. 5

NOVEMBER 1960

Price Rs. 2 or 3 Sh. Annual Subscription Rs. 18

PRINTED AT THE LUCKNOW PRESS, BANGALORE CITY, BY T. R. BALAKRISHNAN,
SUPERINTENDENT, AND PUBLISHED BY THE INDIAN ACADEMY OF
SCIENCES, BANGALORE.

THE LUMINESCENCE SPECTRA OF DIAMOND

By A. Jayaraman, F.A.Sc.

(*Memoir No.* 124 *from the Raman Research Institute, Bangalore-6*)

Received October 24, 1960

1. Introduction

The luminescence of diamond has been the subject of numerous investigations in the past and these have principally dealt with two types of emission spectra commonly met with, one lying in the blue and the other in the yellow-green regions of the spectrum. P. G. N. Nayar[1] made a detailed study of the former while the latter was first extensively studied by Miss Anna Mani.[2] The latter author investigated both the emission and absorption spectra of several fluorescent diamonds at room temperature and at 80° K. The principal features in the spectra of the blue luminescent diamonds are that at 80° K., a line at λ 4152 A.U. appears in emission as well as in absorption, accompanied by a set of bands arising out of the combination of the electronic frequency with the lattice vibrational modes of the crystal. These bands appear in emission on the longer wavelength side, while in absorption they lie on the shorter side. In the case of diamonds exhibiting a greenish-yellow luminescence, a sharp line at λ 5034 A.U. appears, accompanied by vibrational bands. Apart from these, Miss Mani reported the occurrence of numerous sharp electronic lines in the fluorescence spectrum of diamonds. Recently, Dyer and Mathews[3] have studied fluorescence spectra of several diamonds at liquid-air temperature, and report in addition to the above-mentioned two emissions, an electronic line at λ 6100 A.U. and a band system associated with it. They have also investigated luminescence spectra of irradiated and heat-treated diamonds. Gomon[4] reports studies on diamonds of Russian origin.

Several years ago, a set of uncut diamonds of South African origin were acquired by Professor Sir C. V. Raman and added to his impressive collection of nearly five hundred diamonds. Some of these newly acquired diamonds exhibited unusual types of fluorescence when exposed to near ultraviolet radiation. The spectra of these were recorded at room temperature, as far back as 1951 by the present writer and was reproduced in an article by Sir C. V. Raman in *Current Science*.[5] These, however, did not reveal any

noteworthy features, except broad lines and unresolved bands superposed on a continuum. The recent acquisition of a liquid-air plant by this Institute enabled a study of the spectra of these diamonds to be made at liquid-air temperature. A number of other diamonds from the collection were also re-examined. These studies have revealed several interesting facts and some new features in addition to those briefly set out in the preceding paragraph. Three hitherto unrecognised strong electronic emission lines with associated band systems have been observed during the present investigation, namely, those located at λ 4958, λ 5106·38 and λ 5786. Numerous other electronic lines have also been recorded. The important question of the origin of luminescence in diamond will be discussed later in the light of the knowledge accumulated during recent years on the structure and physical properties of this fascinating substance.

2. MATERIALS AND METHODS

In all, spectra of over twenty diamonds were recorded both at room temperature (300° K.) and at 80° K. Eight uncut diamonds of South African origin declared as industrial quality were studied. They all belong to the strongly luminescing class. Many of these are free from any body colour and are clear crystal fragments, while a few are found to possess a light yellow body colour. Four of the specimens were beautiful octahedral crystals of South African origin, exhibiting blue luminescence of varying intensity. Another set of four well-crystallised diamonds, having curved edges, were from the State of Panna in Central India. These exhibited either a weak blue or greenish-blue luminescence. A batch consisting of four diamonds were cut gems exhibiting intense luminescence, the colours being respectively blue, green, bluish-green and bluish-white. In Table I are listed the diamonds which have been studied for the first time. The colour of luminescence and the principal emission lines observed in them are also given in Table I.

A Hanovia high-pressure quartz mercury arc was used for the excitation of fluorescence. The radiation after passing through a Wood's glass filter which cut off all wavelengths higher than 4046 A.U. was focussed on the diamond under investigation. The 3650 group of lines were the principal source for the excitation of fluorescence. For low temperature studies, the diamond was embedded in Wood's alloy filled in a small cavity formed in a copper block which was soldered to one end of a brass tube, one inch in diameter and about twelve inches in length. This arrangement had a pyrex glass envelope, the space between which was evacuated with a two-stage

TABLE I

No.	Shape	Body colour	Colour of luminescence	Observed emission systems
D 1	Irregular	No body colour	Orange	5786·27, 5898·88
D 2	,,	,,	Lemen yellow	4152 v.w., 5034 s.
D 3	,,	,,	Golden yellow	5034 v., 5018
D 4	,,	,,	Yellowish-white	4152 s., 5034 s., 5106 s.
D 5	,,	,,	Violetish-white	4152 s., b., 5034 s., 5106
D 6	,,	,,	Bright blue	4152 s., v.b., split into two
D 7	,,	,,	Whitish	4152 s., b., 5034 s.
D 60	Cut diamond	Colourless	Bluish-green	4152 s., b., 4958 v.s., 5031·5 s.
D 54	Cut diamond gem	,,	Bright blue	4152 s., b., split into two
D 52	,,	Greenish	Bright green	4152 v.s., v.b., split, 4958 v.s., v.b., 5034 self-reversed
D 178	Cut diamond	Colourless	Bluish-white	4152 v.s., v.b., 5034 v.w.

s., strong; v.s., very strong; v.w., very weak; b., broad; v.b., very broad.

rotary pump. A joint at the top was secured by flanges on the brass and glass tubes. The flanges had ground flat surfaces and DC 4 silicon grease was used between the two flanges to obtain a vacuum-tight seal. With this arrangement and maintaining a vacuum of 0·1 mm. of mercury, each liquid-air filling lasted for about 30 minutes. The glass envelope had flat windows at appropriate places for the ultra-violet radiations to enter and for the fluorescent radiations to come out. The latter was focussed on to the slit of a two-prism Huet spectrograph having an aperture of F 4·7. Spectra of strongly luminescent diamonds could be recorded intensely with this arrangement in about an hour's time, using Ilford H.P.S. plates. It took three to four hours to record weakly fluorescent diamonds. The H.P.S. plates, although possessing high speed, are poor in contrast and resolution. Photographing the spectra either with Ilford special-rapid or Process-Panchromatic plates was found to be highly satisfactory and rewarding, as the plates then

revealed far more detail, although these plates demanded a four or even five-fold increase of exposure time.

3. EXPERIMENTAL RESULTS

The majority of diamonds exhibit a blue luminescence, the intensity however being highly variable. A green or yellowish-green luminescence is also met with not infrequently. A golden yellow or orange luminescence is somewhat rarer and especially the latter. One diamond in our collection shows an orange luminescence. A sensible increase in the intensity of luminescence is noticeable when diamonds are cooled down to 80° K. Another fact of observation worthy of mention is that the luminescence of diamonds which exhibit a white colour at room temperature turn distinctively yellowish when the diamond is cooled. Eight typical spectra recorded at 80° K. are reproduced in Fig. 1. A critical study of these reveals that five electronic emission lines occurring at λ 4152, λ 4963, λ 5034, and λ 5786 are prominent features. These are accompanied by vibrational bands and the colour of luminescence is largely dependent on which of the above principal emission line is the strongest. Accordingly, the blue luminescent diamonds show the λ 4152 emission line very strongly, the green ones the λ 4963 line, the greenish-yellow variety the λ 5034 or the λ 5106 line, while in golden yellow and orange luminescent diamonds the λ 5786 comes out with great intensity. In diamonds exhibiting an almost white, yellowish-white or bluish-white luminescence, both the 4152 and 5034 lines appear in equal strength. Some diamonds show exclusively one of these lines only.

λ 4152 *Emission*.—A great many diamonds exhibit this line in varying degrees of sharpness and intensity. In strong blue luminescent diamonds, the line is very intense and very broad and appears as a doublet with a dark line in the centre. This character is observable, if studies are made with thick crystals and arises due to self-reversal of the λ 4152 emission. In Fig. 1 (*f*) which is the spectrum of D 54, this feature can be clearly seen; In Figs. 1 (*a*) and 1 (*b*) which are spectra of D 4 and D 60 respectively, this line has come out with a fair degree of sharpness. It was thought that a non-birefringent diamond, exhibiting a weak blue luminescence might give a very sharp λ 4152 line. D 56 which is a natural octahedral cleavage plate showing no birefringence and of weakly blue luminescent class was chosen. The spectrum however showed that the λ 4152 line is no more sharper than that observable in the two above-mentioned diamonds.

λ 4958, 5034 and 5106·38 *Emissions*.—In bluish-green and green luminescent diamonds the λ 4963 line comes out strongly. The luminescence

spectra of D 60 and D 52 which exhibit respectively a bluish-green and green luminescence are reproduced in Figs. 1 (*b*) and 1 (*e*). In the latter diamond, λ 4958 is the strongest and is very broad and diffuse even at 80° K. Diffuse bands also occur on the longer wavelength side. This line which comes out strongly in the three examples is also accompanied by a sharp line at λ 5031·16. In D 60 this line is of comparable intensity and therefore a band system associated with this electronic frequency also comes out and is overlapping the bands excited by λ 4963. In Fig. 2 (*c*) an enlarged spectrum of D 60 is reproduced. The spectrum of D 4 is also reproduced for purposes of comparison.

The 5034 and 5106 emission lines occur invariably together. The former is always found to be more intense than the other and is the strongest line in greenish-yellow diamonds. With diamonds in which these emissions appear along with the 4152 radiation in more or less equal strength, the colour of luminescence is almost whitish. In Figs. 1 (*a*), 1 (*c*) and 1 (*g*), the spectra of such diamonds are reproduced. Of these, the spectrum of D 4 exhibits numerous sharp electronic lines apart from the sharp λ 4152, λ 5034 and λ 5106 lines which dominate the spectrum. Figure 2 (*b*) is an enlarged photograph of the luminescence spectrum of this diamond. In Fig. 2 (*a*), a highly enlarged photograph of the λ 4152 emission line and the band system associated with it is reproduced. In Fig. 4, a microphotometer record of this portion of the spectrum appears. Figure 5 reproduces the microphotometer record of the λ 5034 and λ 5106 emissions and associated bands. In Fig. 3, the microphotometer record of the entire region between 4152 and 5200 A.U. of the spectrum of D 4 is reproduced. Some of the sharp electronic frequencies falling between λ 4152 and λ 5034 can be seen clearly in the record. A unique feature of this diamond is the occurrence of a sharp electronic line at λ 4403, next to the sharp edge of the band system. In Fig. 1 (*d*) which is the spectra of a lemon yellow luminescent diamond (D 2), numerous sharp electronic lines appear, but they are not so clear in the print.

The width of the lines is found to be variable and it can be said that it usually follows the general intensity of luminescence. The more the intensity of fluorescence, the broader are the lines.

λ 5786 *Emission.*—One of the diamonds in our collection has a projecting tip which exhibits an orange luminescence. The spectrum of this recorded at 80° K. is reproduced in Fig. 1 (*h*). The wavelength of the line corresponds to λ 5786·27 and this is accompanied by a set of bands on the longer wavelength side. In the spectrum of this diamond may be found

other sharp electronic lines. The main body exhibits a faint blue luminescence and therefore the λ 4152 line is also recorded in the spectra of this diamond.

A comparison of the spectra of several diamonds recorded at room temperature and at 80° K. reveals that in general the electronic lines in all cases get sharpened and the bands appear better resolved on cooling. Such an effect is highly pronounced for lines occurring at wavelengths greater than 4400 A.U. In spectra recorded at room temperature, the line character of the electronic frequencies is hardly visible. Except the 4152 emission which appears as a very broad line shifted slightly towards longer wavelength, the line character of the electronic frequencies is hardly noticeable. The longer the wavelength at which the electronic lines occur, the more pronounced is the effect of temperature on the width of the line.

THE LATTICE SPECTRUM OF DIAMOND

In Table II are listed all the electronic frequencies observed. The more intense among these which are followed by a band system are italicised.

TABLE II

Diamond number and colour of luminescence		Electronic lines Wavelength in A.U.
D 4	Yellowish-white ..	*4152·59*, 4403·03, 4577·2, 4597·3, 4789·86, 4850·74, 4860·95, 4876·82, 4889·84, 4967·0, 5018·1, 5027·1, *5034·02*, *5106·38*
D 60	Bluish-green ..	*4152·59*, 4906·86, *4958·55*, 4981·03, *5031·16*, 5042·5, 5374·50, 5749·29, 5806·53
D 2	Lemon yellow ..	4152·49, 4402·08, 4615·98, 4494·29, 4635·54, 4737·61, 4790·21, 4889·25, *5034·81*, 5106·24
D 3	Golden yellow ..	4152·57, *5034·55*, 5106·69, 5179·87, 5232·23, 5245·57, 5786·27
D 1	Orange ..	5034·22, 5107·48, 5704·54, 5733·38, 5762·80, *5786·27*, 5822·65

The frequency shifts measured in wave-numbers of the bands are given separately in Table III.

TABLE III

Mode No.	Degeneracy	Frequency shift (evaluated)	Frequency shift observed in the luminescence spectrum
I	3	1332	1331·91
II	8	1250	1246·23
III	6	1239	..
IV	4	1149	1155·69
V and VI	3+3	1088	1090·8 1064·6
VII	4	1008	1007·09
VIII	6	740	750·0
IX	8	621	..

With D 4, the bands have resolved very well and the microphotometer record reproduced shows the peaks much more prominently and convincingly than those published earlier. The frequency shifts in wave-numbers are noted in the figure. The frequency shifts represent the vibration frequencies of the diamond lattice and much has been written about them in the earlier publications.

A detailed theoretical analysis of the vibration spectrum of the diamond lattice, based on Raman's theory of crystal dynamics, leads to the evaluation of frequencies of the diamond structure[6] and accordingly eight frequencies should be observable. Of these the principal mode of vibration with the frequency shift 1332 cm.$^{-1}$ appears in the first order Raman spectrum. The rest of the frequencies do not appear in the first order Raman spectrum, but appear as octaves and combinations in the second order Raman spectrum of diamond. However, in the luminescence spectrum, the electronic frequency combines with these frequencies and gives rise to the vibration spectrum.

The positions of the peaks correspond to the frequency shifts worked out and in Table III are given the evaluated frequencies and those obtained from a measurement of the shifts of the vibration frequencies observable in the luminescence spectrum. The latter represent oscillations of the diamond lattice with discrete frequencies, lending full support to the correctness of crystal dynamics developed by Prof. Raman. In Figs. 2, 3 and 4, the lattice spectrum can be clearly seen and the respective frequency shifts are inserted in the figures.

The author wishes to express his sincere thanks to Professor Sir C. V. Raman, F.R.S., N.L., for the continued interest he showed and the constant encouragement he gave during the course of this investigation.

SUMMARY

The communication reports the results of study of the luminescence spectra of diamonds recorded at liquid-air temperature (80° K.). Apart from the two well-known electronic frequencies at λ 4152 and λ 5034 and the associated band systems, the present study has revealed the existence of three new electronic emissions centred at λ 4958, λ 5106 and λ 5786 which come out with great intensity along with the vibrational bands excited by them. Numerous sharp electronic lines also appear in the spectrum of some of the diamonds.

Greatly improved records of the vibration spectrum associated with the λ 4152 emission have been obtained and the vibration frequencies deduced from them agree closely with the frequencies evaluated on the basis of Raman's theory of lattice dynamics. The investigation reveals that the λ 4152 emission, λ 4958, λ 5034 and λ 5786 emissions can exist independently and the colour of luminescence is dependent on which of these emissions is the principal feature of a particular diamond. In diamonds exhibiting a white luminescence λ 4152 and λ 5034 emissions appear in equal strength. The effect of temperature on the sharpening of the electronic frequencies is found to be more for emissions occurring at greater wavelengths.

REFERENCES

1. Nayar, P. G. N. .. *Proc. Ind. Acad. Sci.*, 1941, **13 A**, 284, 483, 534; **14 A**, 1.
2. Miss Anna Mani .. *Ibid.*, 1944, **19 A**, 231; **20 A**, 117.
3. Dyer, H. B. and Matthews, I. G. *Proc. Roy. Soc.*, 1957, **243 A**, 320.
4. Gomon, G. O. .. *Optics and Spectroscopy*, 1960, **8**, 275.
5. Raman, Sir C. V. .. *Curr. Sci.*, 1950, **19**, 359.
6. ——— .. *Proc. Ind. Acad. Sci.*, 1956, **44 A**, 99.

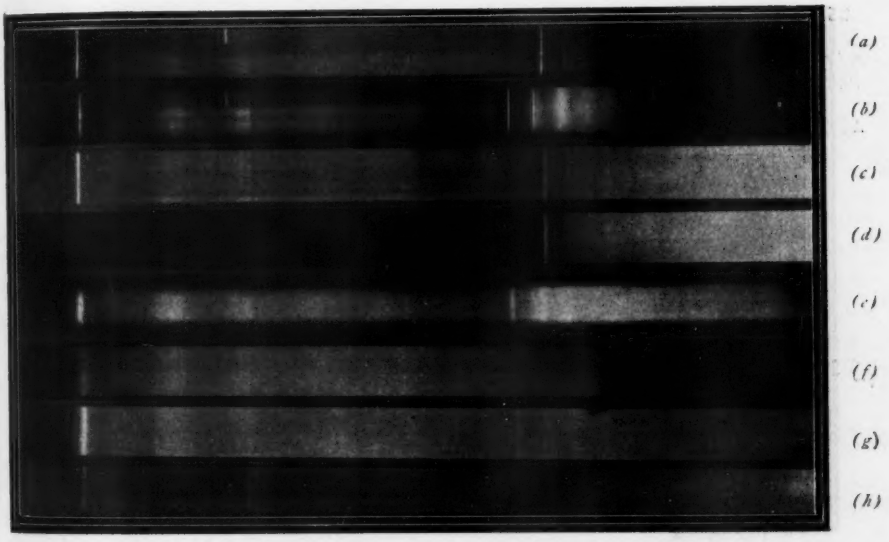

FIG. 1. Luminescence Spectra of Diamonds Recorded at 80° K.

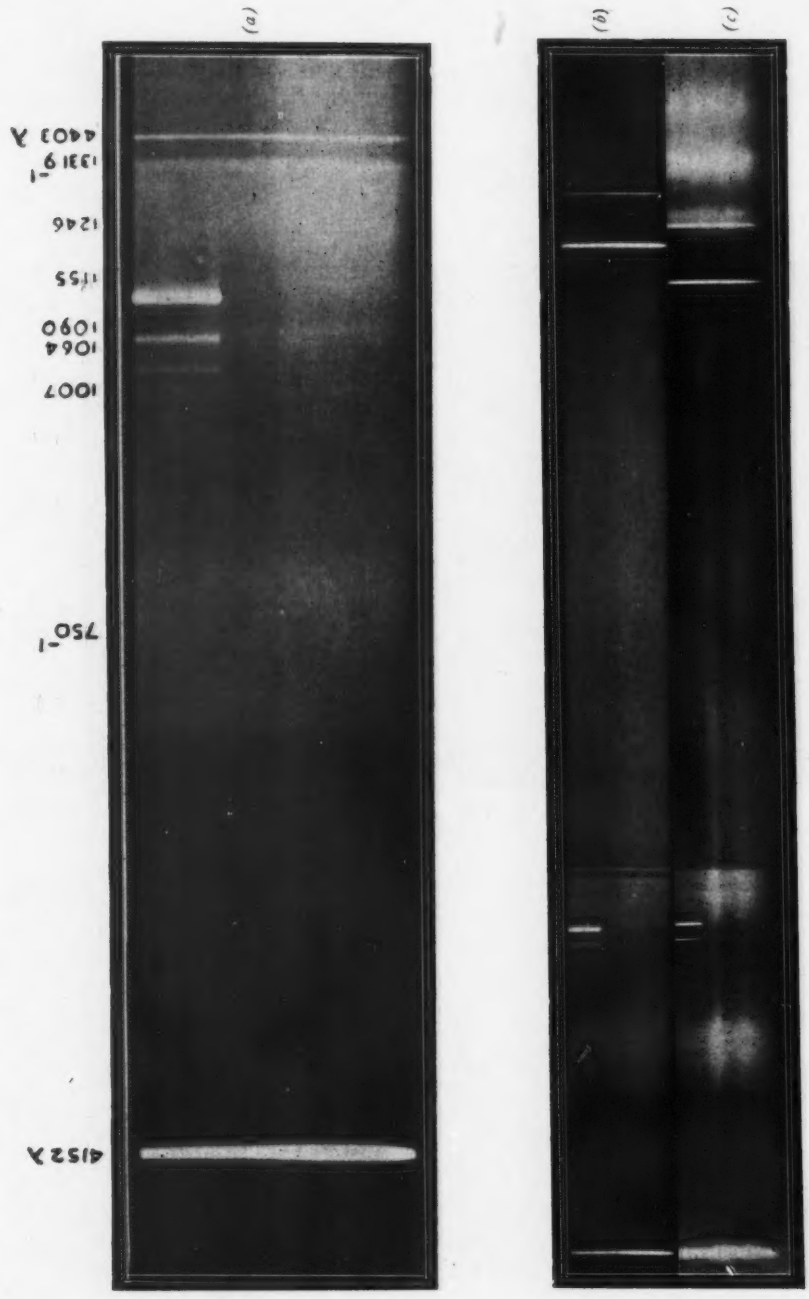

FIG. 2. (*a*) Enlargement of a portion of Fig. 1 (*a*); (*b*) Enlargement of Fig. 1 (*a*); (*c*) Enlargement of Fig. 1 (*b*).

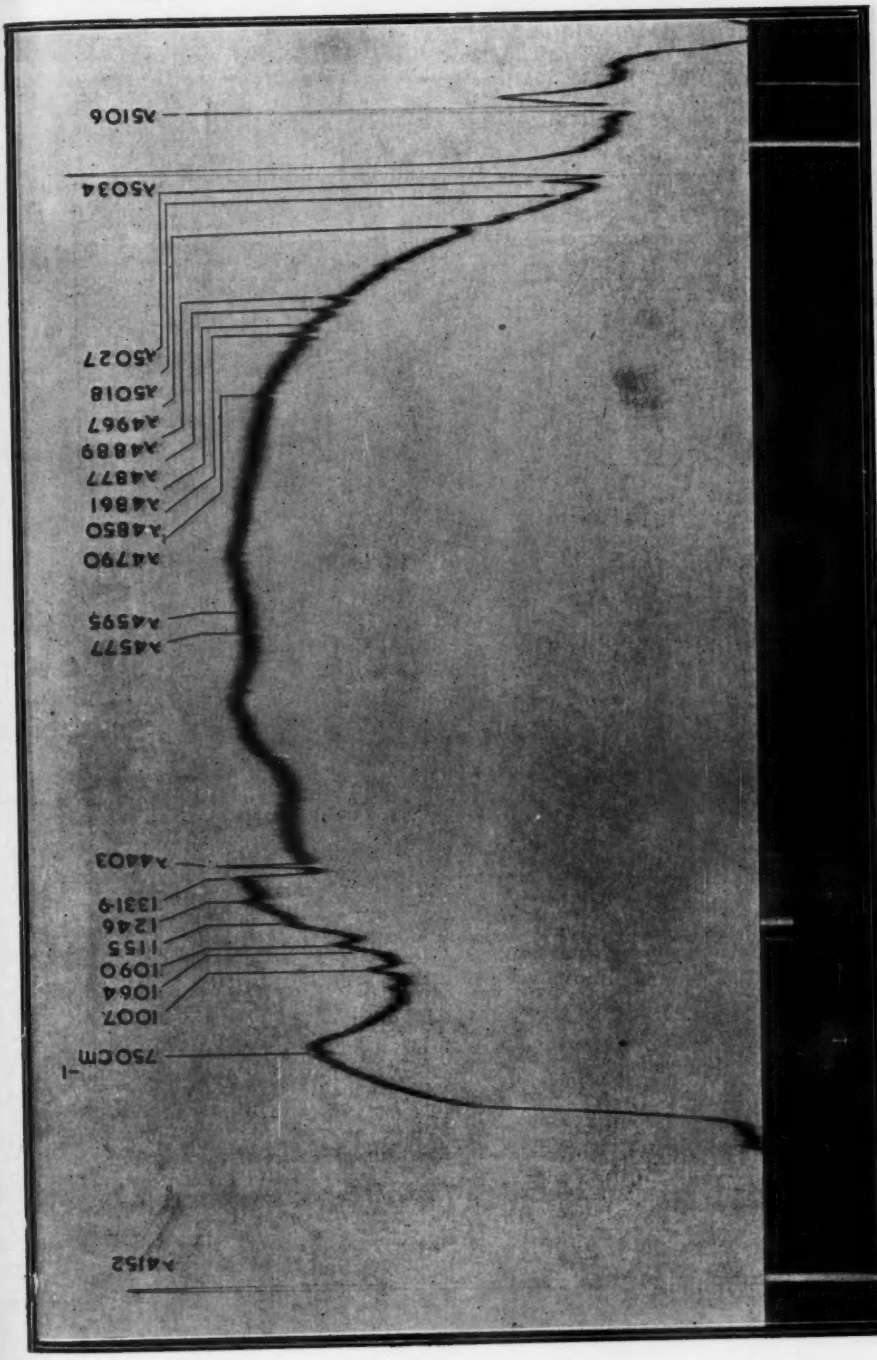

FIG. 3. The Luminescence Spectrum of Diamond and its Microphotometer Record.

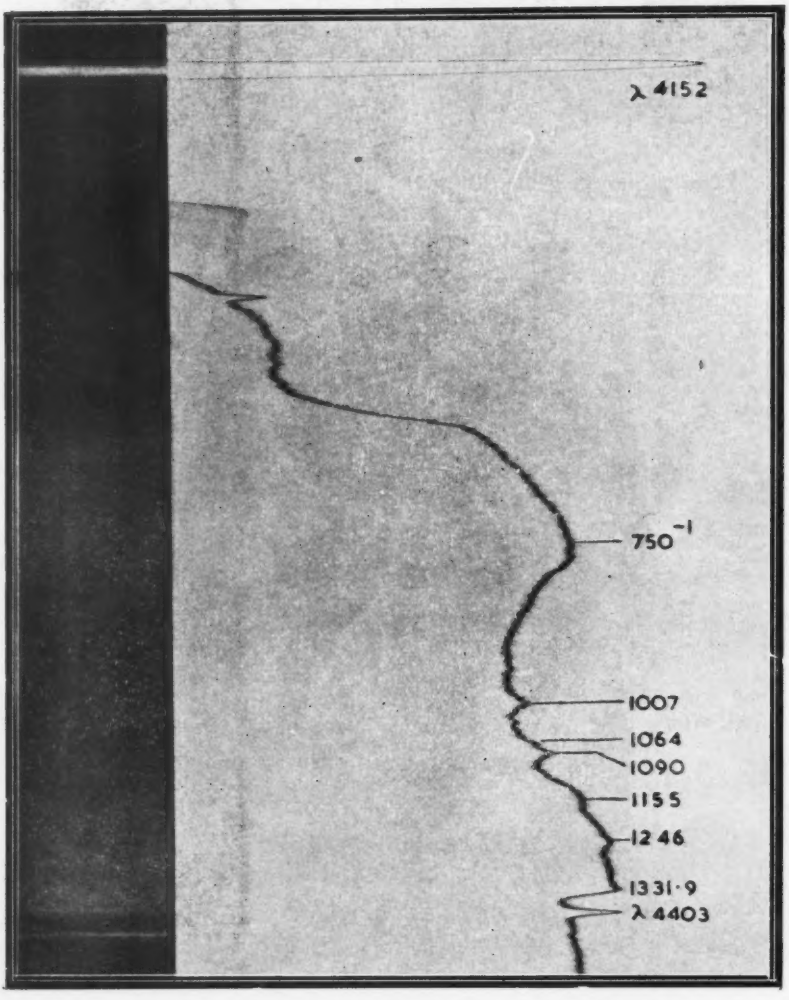

FIG. 4. The 4152 Electronic Line and the Vibration Spectrum accompanying it.

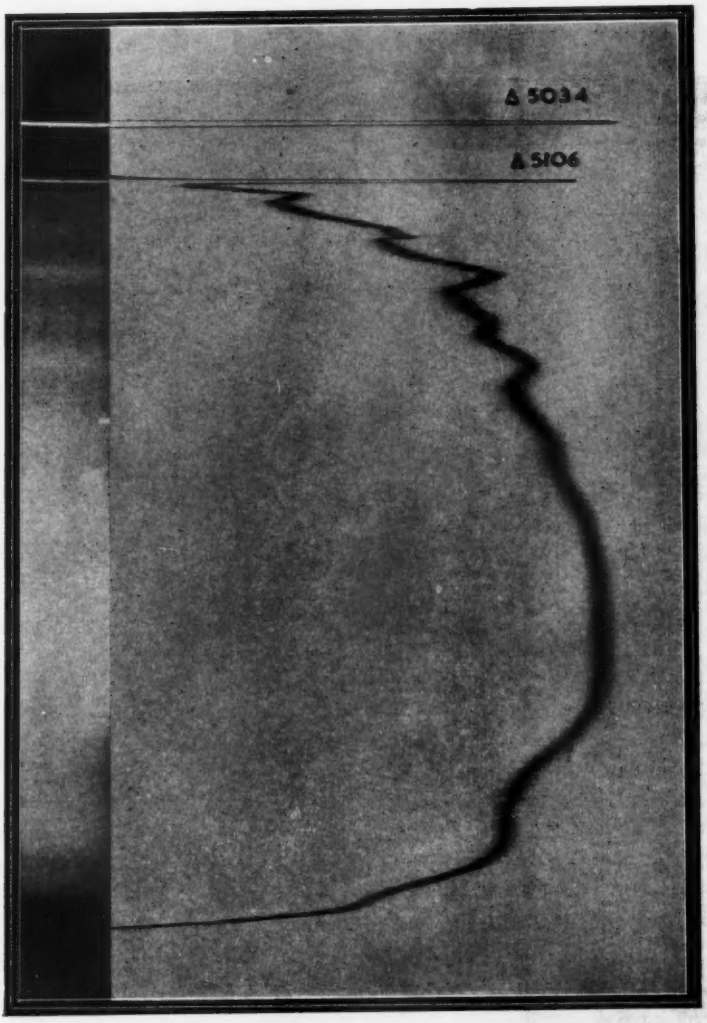

FIG. 5. The 5034 and 5106 Electronic Lines and the Vibration Spectrum accompanying them.

CONDUCTOMETRIC DETERMINATION OF A FEW PHYSICO-CHEMICAL CONSTANTS OF MUREXIDE

By N. A. Ramaiah and R. K. Chaturvedi

(*Department of Physical Chemistry, National Sugar Institute, Kanpur*)

Received June 29, 1960

(Communicated by Prof. S. N. Gundu Rao, F.A.SC.)

Murexide (I) or the ammonium salt of purpuric acid (NH_4P) was discovered by Prout (1818)[1] during the development of test for detection of uric acid. Hantzsch and Robinson[2] made elaborate attempts to prepare murexide in

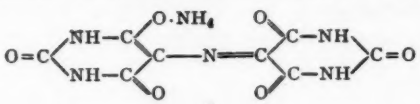

I

a pure state. Davidson[3] described in detail the method of preparation of murexide from alloxantin. Murexide is a reddish-brown shining crystalline substance.

In recent years, attention of a number of research workers has been drawn towards the use of murexide as metal ion indicator and as an analytical reagent. Swarzenbach and co-workers[4] were the first to describe the use of murexide as an indicator for the titration of Ca^{++} with commercial chelating agents such as ethylene-diamine-tetra-acetic acid (EDTA). This marked the advent of development of series of analytical methods for estimation of Ca^{++} in various technical products such as pharmaceutical preparations, textile and sugar-house products. Flaschka[5] gave a review with 23 references on the use of EDTA and murexide in titrations of both cations and anions. Specific directions are given for estimation of Ca^{++} in presence of Mg^{++}, Zn^{++}, Bi^{+++}, Hg^{++}, Al^{+++} and PO_4^{---} in pharmaceutical preparations. Engel[6] described the method for estimation of combined quantities of Ca^{++} and Mg^{++}. Brunisholz[7] used murexide, in presence of magnesium chloride, as an indicator in determination of fluoride with cerium chloride. A method for the estimation of Ca^{++} in sugar-house products has been recently reported from this laboratory.[8]

Williams and Moser[9] have developed a spectrophotometric method for estimation of Ca^{++}. Murexide exhibits absorption maximum at $\lambda = 522\ m\mu$ in the visible region. When added to a solution containing Ca^{++} murexide

combines with Ca^{++} to form a complex with characteristic absorption maximum at $\lambda = 505\ m\mu$. The magnitude of extinction coefficient at this wavelength gives a measure of the amount of Ca^{++}.

No data exist in literature on physico-chemical constants such as ionic mobility, diffusion coefficient and ionic radius of purpurate ion and dissociation constant of murexide. The present paper reports conductometric studies on determination of these constants.

EXPERIMENTAL

Murexide of B.D.H. quality was used; this was purified by the method described by Davidson[10] to obtain a sample of 99·9% purity. Solutions of murexide of desired strength were prepared in double distilled water (specific conductance $1{\cdot}0\times10^{-6}$). The conductance measurements were made with Serfass conductivity bridge S. No. 3638 using a cell with the corresponding constant of 0·218; conductivity measurements were made at $30 \pm 0{\cdot}05°$ C.

SYMBOLS USED

S	= Specific conductance
Λ	= Equivalent conductance
Λ_0	= Equivalent conductance at infinite dilution
Λ'	= Equivalent conductance of free ions
C	= Concentration in formalities
α	= Degree of dissociation
A and B	= Onsager constants
A'	= Debye-Huckel constant
η	= The viscosity of the medium
ϵ	= Dielectric constant
T	= Absolute temperature
e	= Electronic charge
$a°$	= Ionic paramcter in angstrom units
N	= Avogadro Number
B_1	= Constant of the Robinson and Stokes' equation
k	= Boltzman constant
K	= Thermodynamic dissociation constant
K'	$= (A + B\Lambda_0)$

κ = Debye-Huckel parameter
k_0 = Classical dissociation constant from Ostwald's dilution law
f = Activity coefficient
Z = Charge of the ion
μ = Ionic strength
λ_0 = Limiting ionic mobility
F = Faraday
r_s = Ionic radius from Stokes' law
r = Real ionic radius
R = Gas constant
D = Diffusion coefficient

Results

Table I gives a typical set of results on the conductivity of murexide solutions at different concentrations. It may be pointed out that the conductivity measurements were made immediately after the preparation of

Table I

Conductance of murexide solutions at 30·0° *C.*

Concentration $\times 10^3$ M	Specific conductance	Equivalent conductance	Dissociation constant from Ostwald's law
3·28	16·11	107·40	2·06
3·19	15·73	107·66	2·05
2·85	14·13	108·15	1·91
2·80	13·93	108·64	1·96
2·36	11·83	108·61	1·81
1·58	8·17	112·74	1·70

the solutions for the following reasons: Murexide in aqueous solution undergoes decomposition[11, 12] in the pH range of 1–3 and 9–12. This is accompanied by a change in the conductivity of the solution. The decomposition and the corresponding change in the conductivity were, however, inappreciable at pH-6 which corresponds to the pH of the murexide solutions.

Nevertheless, conductometric studies made immediately after the preparation of the solutions gave data of reproducible and reliable nature.

Figure 1 represents the variation of Λ with square-root of concentration (*see* below). Extrapolation of the straight line to y-axis gave a value of

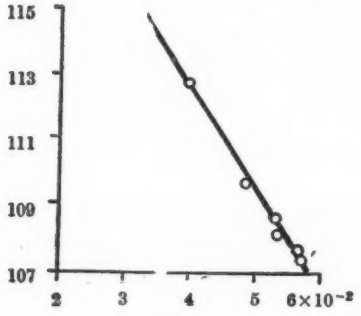

FIG. 1

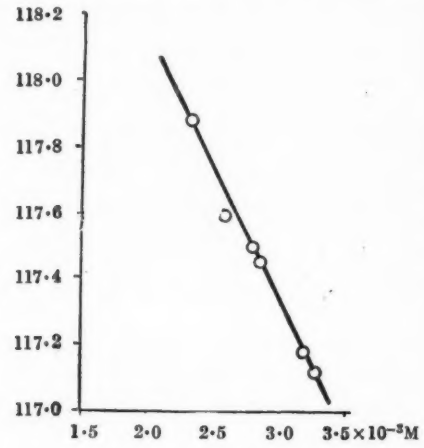

FIG. 2

122·37 mhos. cm.^{2} for Λ_0. This was employed for the computation of α to give k_0 by the familiar equation.

$$k_0 = \frac{\alpha^2 C}{(1-\alpha)}. \tag{1}$$

These data are given in column 4 of Table I. It is seen that k_0 does not remain constant indicating the inapplicability of Ostwald's dilution law to the solution of murexide which behaves presumably as a strong electrolyte.

For strong electrolytes Onsager derived the following equation:

$$\Lambda = \Lambda_0 - (A + B\Lambda_0)\sqrt{C}. \tag{2}$$

It is of interest to note from Fig. 1 that as required by equation 2, Λ is linearly variant with $\sqrt{C}$. The slope of the line gives $(A + B\Lambda_0)$. Here

$$A = \frac{82{\cdot}5}{\eta(\epsilon T)^{1/2}} \quad \text{and} \quad B = \frac{8{\cdot}2\times 10^5}{(\epsilon T)^{3/2}}. \tag{3}$$

For computation of Λ_0 from the slope, the following were used:—

Dielectric constant[13] (ϵ)	76·77
Viscosity[14] (η)	0·80
Temperature (T)	303·0° A
'A'	67·55
'B'	0·231

The value of Λ_0 obtained from the slope of the plot in Fig. 1 differed widely from the value of 122·37 mhos. cm.^{2}/mole^{-1} for Λ_0 obtained as the intercept of the plot (*see* Equation 2). Similar observations have been recorded with number of salts in mixed solvents.[15, 16] These studies suggest that the number of ions contributing to conductivity of the solution is less than the total number obtainable by the dissociation process, which is due presumably to the existence in the system of associated ion-pairs.

5. Ion-Association and Dissociation Constant

For computation of the dissociation constant of a system in which ion-association is marked, the following methods have been found useful:—

(i) Davies Method,[17]

(ii) Robinson and Stokes' Method,[18]

(iii) Brock's method.[19]

The applicability of these methods for the calculation of the dissociation constant of ammonium purpurate was examined in the following:—

5.1. *Davies Method*

According to this method α at a particular concentration is given by the ratio of the equivalent conductance of a system to the corresponding equivalent conductance with no association (Λ'). Here

$$\Lambda' = \Lambda_0 - (A + B\Lambda_0)\sqrt{\alpha C}. \qquad (4)$$

The values of Λ' at different concentrations were calculated by the method of successive approximation. These are given in column 3 (Table II). The degree of dissociation and *pk* values computed from these results are given in columns 4 and 5 (Table II).

TABLE II

Calculation of classical dissociation constant by Davies method

Concentration $\times 10^3$ M	Equivalent conductance of free ions	Degree of dissociation	Classical dissociation constant	*pk*
3·28	117·12	0·9170	3·32	1·479
3·19	117·18	0·9187	3·31	1·480
2·85	117·47	0·9208	2·99	1·520
2·80	117·49	0·9246	3·25	1·500
2·36	117·88	0·9298	2·90	1·537
1·58	118·65	0·9503	2·87	1·540
		pk	1·51±0·03	

5.2. *Robinson and Stokes' Method*

Onsager and Fuoss[20] observe that

$$\Lambda = \Lambda_0 - (A + B\Lambda_0)\sqrt{C} + EC \log C + FC. \tag{5}$$

Equation 5 was found to give satisfactory results only up to concentrations $\geqslant 0{\cdot}01$ N. The constants E and F are to be empirically determined. It may be pointed that the influence of time of relaxation[21] and of electrophoretic effect on the dissociation of a salt are to be considered:—

The relaxation effect[22] can be represented as

$$\frac{\Delta X}{X} = \frac{-e^2}{3k\epsilon T} \cdot \frac{0{\cdot}2929}{1 + a\kappa} \cdot \frac{e^{0{\cdot}2929a\kappa} - 1}{0{\cdot}2929a\kappa} \cdot \tag{6}$$

The last term $e^{0{\cdot}2929a\kappa} - 1/0{\cdot}2929a\kappa$ in Equation 6 can be neglected for the values of $a\kappa < 0{\cdot}3$. Further, in the above equation, κ is given by

$$\kappa = \frac{(8\pi Ne^2)^{1/2}C^{1/2}}{(1000\epsilon kT)^{1/2}} \left\{1 - \frac{1}{2}\frac{n_1}{N_1} - \frac{1}{2}\frac{n_2}{N_2}\right\} \tag{7}$$

where n_1 and n_2 denote the concentration of cations and anions per c.c. and N_1 and N_2 are the number of " sites " per c.c. available to these ions. κ is also given by

$$\kappa = \frac{(8\pi Ne^2)^{1/2}C^{1/2}}{(1000\epsilon kT)^{1/2}} \cdot \tag{8}$$

The difference between the values of κ from Equation 7 and from Equation 8 arises from the fact that in the derivation of Equation 7 distribution function[23] other than the Boltzman function has been employed. As pointed out by Wishaw and Stokes,[24] the derivation of the correction factor in Equation 7 (*cf.* Equation 8) by Falkenhagen *et al.*[22] using Eigen-Wicke distribution function[23] instead of the usual Boltzman distribution, is of doubtful validity. The value of κ as given by Equation 8 is therefore used for estimating the relaxation (and electrophoretic) effect (*see* below).

The influence of electrophoretic effect is given by the expression[24]

$$-\left(\frac{82 \cdot 5C^{1/2}}{\eta(\epsilon T)^{1/2}}\right)(1 + a\kappa). \tag{9}$$

Combining the electrophoretic effect (Equation 9) and the relaxation effect (Equation 6) using the value of κ from Equation 8, the following equation for Λ of univalent electrolytes of non-associated type, is obtained

$$\Lambda = \left(\Lambda_0 - \frac{A\sqrt{C}}{1 + B_1 a^\circ \sqrt{C}}\right)\left(1 - \frac{B\sqrt{C}}{1 + B_1 a^\circ \sqrt{C}}\right). \tag{10}$$

The constant B_1 is given by

$$B_1 = \frac{50 \cdot 29}{(\epsilon T)^{1/2}} \cdot \tag{11}$$

For systems involving ion-association, the concentration of free ions will be αC instead of C. Substituting in place of C in Equation 10 we get

$$\Lambda' = \left(\Lambda_0 - \frac{A\sqrt{\alpha C}}{1 + B_1 a^\circ \sqrt{\alpha C}}\right)\left(1 - \frac{B\sqrt{\alpha C}}{1 + B_1 a^\circ \sqrt{\alpha C}}\right) \tag{12}$$

where

$$\alpha\Lambda' = \frac{\Lambda\eta}{\eta_0}. \tag{13}$$

The term η/η_0 gives the viscosity correction which is insignificant at low concentrations investigated and therefore omitted.

In order to calculate Λ' a suitable value is to be assigned to $a°$. It may be added that ion-pair formation will take place only when the sum of the effective radii of the ions is less than Bjerrum's critical distance of 3·57Å. For free ions, $a°$ can therefore, be assumed to be equivalent to or greater than 3·57 Å. Employing the minimum value of $a°$, *viz.*, 3·57 Å, the equivalent conductance due to free ions (Λ') at different concentrations was calculated by using Equation 12. These are returned in column 3 of Table III. The value of α and *pk* are given in columns 4 and 5.

TABLE III

Calculation of classical dissociation constant by Robinson and Stokes' method

Concentration $\times 10^3$ M	Equivalent conductance of free ions	Degree of dissociation	Dissociation constant	*pk*
3·28	117·50	0·9135	3·16	1·501
3·19	117·54	0·9159	3·18	1·497
2·85	117·78	0·9182	2·94	1·532
2·80	117·81	0·9221	3·06	1·515
2·36	118·14	0·9278	2·81	1·552
1·58	118·84	0·9486	2·77	1·557
		pk	1·525±0·03	

5.3. *Brock's Method*

An extension of Davies method for evaluation of Λ' (5·1) has been recently developed. For this purpose Equation 4 is rearranged as

$$\Lambda = \alpha\,[\Lambda_0 - (A + B\Lambda_0)\sqrt{\alpha C}\,]. \tag{14}$$

Equation 14 can be represented as a function of the degree of dissociation in the form

$$f(\alpha) = \alpha^{3/2}C^{1/2}\kappa' - \alpha\Lambda_0 + \Lambda = 0. \tag{15}$$

Let α_1' be the first approximation of α so that $\alpha_1 = \alpha + h$, where h is a constant. Expanding $f(\alpha)$ in Taylor's series we obtain

$$f(a) = f(a_1) + hf'(a_1) + \frac{h^2}{2} f''(a_1) + \cdots. \tag{16}$$

Assuming that the third and higher terms are small and negligible, we get

$$h = -\frac{f(a_1)}{f'(a_1)}. \tag{17}$$

so that the second approximation of a_2 becomes

$$a_2 = a_1 - \frac{f(a_1)}{f'(a_1)}. \tag{18}$$

Substituting Equation 15 in Equation 18 and putting $a_1 = \Lambda/\Lambda_0$ we get

$$a_2 = \frac{\Lambda}{\Lambda_0} - \frac{\left(\frac{\Lambda}{\Lambda_0}\right)^{3/2} C^{1/2}\kappa'}{\frac{3}{2}\left(\frac{\Lambda}{\Lambda_0}\right)^{1/2} C^{1/2}\kappa' - \Lambda_0}. \tag{19}$$

The values of a_2 obtained from Equation 19 are given in column 2 of Table IV. Column 3 gives the pk values computed from data in columns 1 and 2.

Reference to data in Tables II to IV indicates that different values of pk obtained by varied methods agree with each other; the average values of these are given in column 2 of Table V.

TABLE IV

Calculation of classical dissociation constant by Brock's method

Concentration $\times 10^3$ M	Degree of dissociation	Classical dissociation constant	*pk*
3·28	0·9122	3·10	1·508
3·19	0·9187	3·31	1·480
2·85	0·9208	3·07	1·513
2·80	0·9242	3·15	1·501
2·36	0·9298	2·90	1·537
1·58	0·9498	2·85	1·546
		pk	1·512 ± 0·03

TABLE V

Classical k *and thermodynamic* K *dissociation constant of murexide*

		pk	*pK*
1. Davies Method	..	1·506 ± 0·03	1·555 ± 0·03
2. Robinson and Stokes' Method	..	1·523 ± 0·03	1·572 ± 0·03
3. Brock's method	..	1·512 ± 0·03	1·556 ± 0·03
Mean value	..	1·514 ± 0·03	1·561 ± 0·03

6. THERMODYNAMIC DISSOCIATION CONSTANT

The thermodynamic dissociation constant of murexide or ammonium purpurate (NH_4P) is given by

$$K = \frac{[NH_4^+]\,[P^-]}{[NH_4P]} \cdot \frac{f_{NH_4^+} \cdot f_{P^-}}{f_{NH_4P}} \tag{20}$$

and is computed employing the following modified Debye-Huckel equation[25] for

$$-\log f_i = \frac{AZ_i^2\sqrt{\mu}}{1+\sqrt{\mu}}. \tag{21}$$

The values of pK obtained are given in column 3, Table V. The data suggest that the dissociation constant of murexide can be considered to be $2{\cdot}75\times10^{-2}$ ($pK = 1{\cdot}56$) which indicates the strongly ionizable nature of ammonium purpurate. It is instructive to compare the dissociation constant of purpuric acid[26]: $k = 1{\cdot}58\times10^{-2}$ ($pk = 1{\cdot}80$).

7. COMPUTATION OF IONIC MOBILITY AND IONIC RADIUS

The linear variation of Λ' with C is shown in Fig. 2. The extrapolation of the straight line to zero concentration gives the value of the equivalent conductance of the free ions at infinite dilution which corresponded to 119·7; λ_0 values of NH_4^+ was computed from the data[22] on the conductivity of NH_4Cl and Cl^-. Simple application of Kohlrausch law gives 38·12 mhos. cm.^{2} for the limiting ionic mobility of purpurate ion.

Assuming that Stokes' law is applicable to the movement of ions under electric field, we have

$$r_s = \frac{0{\cdot}82\,Z}{\lambda_0 \eta}. \qquad (22)$$

Equation 22 gives a value of 2·68 Å for r_s. Stokes' law, however, requires the movement of a particle of macroscopic dimensions in an ideal medium. For the ions with radii less than 5 Å, the values of ionic radius obtained by Equation 5 are reported to be very low and are therefore to be corrected. A factor has been worked out[28] for ions of various sizes. For a value of 2·68 for r, this appeared to be approximately 1·44, leading to an approximate value of 3·88 Å as the real ionic radius of purpurate ion, in close agreement with the corresponding value of 3·4 Å computed from the data on conductivity of purpuric acid[26] obtained at 0° C.

8. Diffusion Coefficient of Purpurate Ion

The conductivity data presented in the previous articles are employed for determining the diffusion coefficient (D) of the purpurate ion on which no data exist in the literature. D is related to the limiting ionic mobility (λ_0) by the following equation due to Nernst[29]

$$D = \frac{RT\lambda_0}{F^2 Z} \qquad (23)$$

λ_0 for the purpurate ion (*see* §7) corresponded to a value of 38·12 mhos.cm.^{2} Substitution of this value in Equation 22 gives a value of $1{\cdot}03 \times 10^{-5}$ cm.^{2}sec.$^{-1}$ for the diffusion coefficient of the purpurate ion.

Summary

Conductance measurements of murexide or ammonium purpurate solutions were made at 30° + 0·05° C. using a Serfass conductivity bridge. Ostwald's dilution law was found to be inapplicable; equivalent conductance at infinite dilution and the classical and thermodynamic dissociation constants were computed by various methods applicable for systems involving ion association. The following physico-chemical constants of murexide were calculated:—

(*a*) Thermodynamic dissociation constant.

(*b*) Ionic mobility of purpurate ion.

(*c*) Ionic rasius,

(*d*) Diffusion coefficient.

9. ACKNOWLEDGEMENT

Authors' grateful thanks are due to Prof. S. N. Gundu Rao, B.Sc., A.H.B.T.I., F.A.Sc., F.R.I.C., Director, National Sugar Institute, for his kind interest in the work; to the Ministry of Scientific Research and Cultural Affairs, Government of India, for a fellowship to one of us (R. K. C.); and to U.P. Scientific Research Committee for a contingency grant.

REFERENCES

1. Prout .. *Phil. Trans.*, 1818, 420.
2. Hantzsch and Robinson .. *Ber.*, 1910, **43**, 92.
3. Davidson .. *J. Am. Chem. Soc.*, 1936, **58**, 1821.
4. Swarzenbach, Biedermann and Bangerter *Helv. Chim. Acta.*, 1946, **29**, 811.
5. Flaschka .. *Scientia pharmac*, 1953, **21**, 126.
6. Engel .. *Das Leder*, 1951, **2**, 241.
7. Brunisholz .. *Helv. Chim. Acta.*, 1937, **37**, 1546.
8. Ramaiah, Vishnu and Chaturvedi *Naturwiss.*, 1958, **45**, 290.
9. Williams and Moser .. *Anal. Chem*, 1953, **25**, 1414.
10. Davidson .. *J. Am. Chem. Soc.*. 1936, **58**. 1821.
11. Ramaiah, Gupta and Vishnu *Zeit fur Naturforsch*, 1957, **126** (3), 189.
12. —— and Chaturvedi .. Unpublished data.
13. Wyman and Ingalls .. *J. Am. Chem. Soc*, 1938, **60**, 1182.
14. Robinson and Stokes .. *Electrolytic Solutions*, Butterworths Publications, London, 1955, 447.
15. Davies .. *J. Chem. Soc.*, 1958, 3660.
16. Nash and Monk .. *Trans. Far. Soc.*, 1958, **54**, 1650.
17. Davies .. *Ibid.*, 1927, **23**, 351.
18. Robinson and Stokes .. *J. Am. Chem. Soc.* 1954, **70**, 1991.
19. Brock .. *J. Electro-chem., Soc.*, 1957, **104**, 128.
20. Onsager and Fuoss *J. Phys. Chem.*, 1932, **36**, 2689.
21. Stokes .. *J. Am. Chem. Soc.*, 1953, **75**, 4563.
22. Falkenhagen, Leist and Kelbg *Ann. Physick*, 1952, **6** (11), 51.
23. Eigen and Wicke .. *Naturwiss*, 1951, **38**, 453.
24. Wishaw and Stokes .. *J. Am. Chem. Soc.*, 1954, **76**, 2069.
25. Guntelberg .. *Z. Physik. Chem.*, 1926, **123**, 243.
26. Hautzsch and Robinson .. *Ber.*, 1910, **43**, 92.
27. *International Critical Table*, VI, 232.
28. Robinson and Stokes .. *Electrolytic Solution*, Butterworth Publications, London, p. 120.
29. Nernst .. *Z. Physik. Chem.*, 1888, **2**, 613; *cf.* Kilthhff and Lingane, *Polarography*, Interscience Publishers, 1952, p. 52.

DEVIATIONS FROM PARALLELISM AND EQUIDISTANCE IN FINSLER SPACE

By Nirmala Prakash and Ram Behari, F.A.Sc.

(University of Delhi)

Received May 20, 1960

Abstract

In the present paper the deviations from parallelism and equidistance are studied for Finsler spaces in Cartan's sense and for Finsler space which is locally Minkowskian. By considering an orthogonal ennuple of hypersurfaces in F_n properties of associate curvature or angular spread vector have been studied.

Introduction

Parallelism and equidistance in classical differential geometry were studied by Graustein (1932); the same notions were studied and extended for Riemannian spaces by R. M. Peters (1935, 1937).

In the present paper the deviations from parallelism and equidistance are studied for Finsler spaces. In first section the study is based on Finsler space in the sense of E. Cartan (1934) and in second section the Finsler space under consideration is as given by A. Kawaguchi (1953, 1956), H. Rund (1954, 1955) and other writers.

Section I

1. In Riemannian geometry the associate curvature or angular spread is defined as the measure of deviation of vectors λ^i from parallelism, and is given by

$$\frac{1}{r} = (g_{ij}\mu^i\mu^j)^{\frac{1}{2}} \tag{1.1}$$

where

$$\mu^i = \lambda^i, k\frac{dx^k}{ds} \tag{1.2}$$

are perpendicular to unit vector λ having λ^i as contravariant component.

The latin indices followed by a vertical bar denote a particular vector.

If we take Finsler space equipped with Euclidean connection, then the associate curvature (angular spread) vector μ^i given by the relation

$$\frac{1}{r^2} = g_{ij}(x, x')\,\mu^i\mu^j \tag{1.3}$$

is perpendicular to unit vector λ, as the co-variant derivative of fundamental tensor $g_{ij}(x, x')$ vanishes. $1/r$ is the measure of the deviation of vector λ^i at a point $\bar{P}(\bar{x}, d\bar{x})$ of a curve C and the vector which has been transported parallelly from $P(x, dx)$ to $\bar{P}$.

If n linearly independent congruences of curves C_k $(k = 1, 2, \ldots, n)$ with tangent vectors $\lambda^i{}_{k_1} = dx^i/ds_k$ are considered, then the associate curvature vectors of the vectors $\lambda_{k_1}{}^i$ with reference to the curves

$$C_l\,(l = 1, 2, \ldots, n, k \neq l)$$

are given by

$$\mu^j{}_{kl_1} = \lambda^i{}_{l_1}\lambda^j{}_{k_1,i}. \tag{1.3 a}$$

This is called the associate curvature vector of the curves C_k with respect to curves C_l and its length

$$\frac{1}{r^2{}_{kl_1}} = g_{ij}(x, x')\,\mu^i{}_{kl_1}\mu^j{}_{kl_1}$$

is called the associate curvature of the curves C_k with respect to C_l.

Since

$$g_{ij}(x, x')\frac{dx^i}{ds_k}\cdot\frac{dx^j}{ds_k} = 1 \qquad (k = 1, \ldots n)$$

vectors $\mu^j{}_{k^1{}_1}$ are perpendicular to $\lambda^j{}_{k_1}$ $(k \neq l)$.

We take n independent families of hypersurfaces S_l defined locally by the equations $f_l(x^1, x^2, \ldots, x^n, x^{1'}, \ldots, x^{n'}) = C_l$ $(l = 1, 2, \ldots, n')$ such that the distance between any two neighbouring points x^i, $x^i + dx^i$ is given as (E. Cartan, 1934)

$$ds = \mathfrak{L}(x, dx) \tag{2.1}$$

$$s_l = \int \mathfrak{L}_l(x, dx). \tag{2.2}$$

These hypersurfaces intersect in n linearly independent congruences of curves C_l whose unit tangent vectors are $\lambda^i{}_{l_1} = dx^i/ds_l$. The family of hyper-

surfaces S_l have $(n-1)$ independent congruences of curves $C_k\,(k \neq l)$ on them and the family of curves C_l are their transversals.[1]

If d_l be the distance measured along a transversal between two hypersurfaces $S_l: f_l = f_l'$ and $f_l = f_l^1 + f_l^0$ (where f_l^0 is of the order Δf_l^1) and logarithmic directional derivative of d_l be taken in the direction of a curve C_k on f_l then this derivative as $Lt.\ f_l^0 \to 0$ is called the distantial spread of the hypersurfaces S_l with respect to the curves C_l measured along C_k and it is denoted by $1/d_{kl}$.

Thus

$$\frac{1}{d_{kl}} = Lt._{\,f_l^0 \to 0} \frac{\partial \log dl}{\partial S_k} \qquad (k \neq l). \tag{2.3}$$

If S_l is the directed arc of an individual curve C_l as defined by the integral (2.2) then

$$df_l = \frac{\partial f_l}{\partial S_l}\, dS_l$$

where $\partial f_l / \partial S_l$ is the directional derivative of f_l in the positive direction of C_l.

Therefore

$$\frac{1}{d_{kl}} = -\frac{\partial \log \left(\frac{\partial f_l}{\partial S_l}\right)}{\partial S_k} \qquad (k \neq l).$$

If $1/d_{kl} = 0$ then $\log (\partial f_l / \partial S_l)$ is constant and $s_l = F(f_l)$ is the common directed arc measured from a fixed hypersurface S_l with congruence of transversals C_l.

Conversely when $1/d_{kl}$ the distantial spread of hypersurfaces S_l with respect to curves C_l in the directions of the curves C_k $(k \neq l)$ vanishes for all points then each pair of hypersurfaces cut equal segments on transversals.

Now

$$f_l\left(x^1, x^2, \ldots, x^n, \frac{dx^1}{dS}, \ldots, \frac{dx^n}{dS}\right) = C_l$$

---

[1] The word transversal does not stand here for the generalisation of orthogonality, it merely indicates the curves which interesct the remaining $(n-1)$ families of curves C_k. $(k = 1, 2, \ldots, n$ $k \neq l)$.

and

$$\frac{\partial f_l}{\partial S_l} = \frac{\partial f_l}{\partial x^i}\frac{dx^i}{dS_l} + \frac{\partial f_l}{\partial x'^i}\frac{dx'^i}{dS_l}$$

or

$$\frac{\partial f_l}{\partial S_l} = f_{l,i}\lambda_{l_1}{}^i + f_{l,i'}\lambda_{l_1}{}^{i'}. \tag{2.4}$$

As s_l is the arc parameter for the transversals C_l, $\lambda_{l_1}{}^i \equiv dx^i/dS_l$ denotes the unit tangent vector to the curve. The dashed suffixes throughout denote the partial derivative with reference to x'^i and $\lambda_{l_1}{}^{i'} = dx'^i/dS_l$.

Now

$$\frac{\partial \log \frac{\partial f_l}{\partial S_l}}{\partial S_k} = \frac{1}{\frac{\partial f_l}{\partial S_l}}\left[f_{l,ij}\lambda_{l_1}{}^i\lambda_{k_1}{}^j + f_{l,i}\lambda^i{}_{l_1,j}\lambda_{k_1}{}^j + f_{l,i'j}\lambda_{l_1}{}^i\lambda_{k_1}{}^j + f_{l,i'}\lambda^i{}_{l_1,j}\lambda_{k_1}{}^j\right]. \tag{2.5}$$

Also

$$f_{l_1,ij}\lambda_{l_1}{}^i\lambda_{k_1}{}^j = \frac{\partial f_{l,j}\lambda_{k_1}{}^j}{\partial S_l} - f_{l,j}\lambda^j{}_{k_1,i}\lambda_{l_1}{}^i. \tag{2.6}$$

Substituting this value in (2.5) and simplifying it we have

$$\frac{\partial \log \frac{\partial f_l}{\partial S_l}}{\partial S_k} = \frac{1}{\frac{\partial f_l}{\partial S_l}}\left[f_{l,i}(\lambda^j{}_{l_1,j}\lambda_{k_1}{}^j - \lambda^i{}_{k_1,j}\lambda_{l_1}{}^j) + \frac{\partial f_{l,j}\lambda_{k_1}{}^j}{\partial S_l} + f_{l,i'j}\lambda_{l_1}{}^i\lambda_{k_1}{}^j + f_{l,i'}\lambda^i{}_{l_1,j}\lambda_{k_1}{}^j\right] \tag{2.7}$$

or from (1.3)

$$\frac{1}{d_{kl}} = \frac{1}{\frac{\partial f_l}{\partial S_l}}\left[f_{l,i}(\mu^i{}_{lk_1} - \mu^i{}_{kl_1}) + \frac{\partial f_{l,j}\lambda_{kl}{}^j}{\partial S_l} + f_{l,i'j}\lambda_{l_1}{}^i\lambda_{k_1}{}^j + f_{l,i'}\lambda^{i'}{}_{l_1,j}\lambda_{k_1}{}^j\right]. \tag{2.8}$$

Thus we conclude that if the difference between the associated curvature vectors $\mu^i{}_{lk_1}$, $\mu^i{}_{kl_1}$ is zero and the 2nd, 3rd and 4th terms vanish the hypersurfaces are equidistant.

In particular if the vector field $\lambda_{l_1}{}^{i}$ is null the last two terms vanish. In this case the hypersurfaces will be equidistant if the sum $f_{l,j}\lambda_{k_1}{}^{j}$ is constant and the vector difference $(\mu^{i}{}_{lk_1} - \mu^{i}{}_{kl_1})$ is zero.

Equation (2.8) reduces locally to equations in Riemannian space as given by R. M. Peters (1935).

From above considerations, we have a necessary and sufficient condition that the hypersurfaces of each family be equidistant with respect to the congruence of curves not contained in them is that the vector $\mu^{i}{}_{kl_1}$ is identical to $\mu^{i}{}_{lk_1}$, $f_{l,j}\lambda_{k_1}{}^{j}$ is invariant with respect to differentiation along their transversals and vectors $\lambda_{l_1}{}^{i}$ are zero ($l = 1, 2, \ldots, n$).

3. E. Cartan (1934) has shown that a curve in Finsler space with Cartesian basis $(\vec{e}_1, \vec{e}_2, \ldots, \vec{e}_n)$ can be chosen so that at any point P we have

$$\vec{e}_i \vec{e}_j = g_{ij}.$$

We also assume that the independent hypersurfaces form an orthogonal ennuple thus

$$\Sigma\, \lambda_{h_1}{}^{i}\lambda_{h_1}{}^{j} = g^{ij}, \quad \lambda_{h_1}{}^{i}\lambda_{k_1 i} = 0 \quad (h \neq k)$$

and

$$\lambda_{h_1}{}^{i}\lambda_{h_1 j} = \delta_j{}^{i}.$$

We define the projection of the derived vector of λ_{h_1} in the direction of λ_{l_1} on λ_{k_1} as

$$\lambda_{h_1 i,j}\lambda_{k_1}{}^{i}\lambda_{l_1}{}^{j} = \gamma_{hkl} \tag{3.2}$$

which are known as Ricci's coefficients of rotation.

Now

$$\mu^{i}{}_{lk_1}\lambda_{l_1 i} = 0 \tag{3.3}$$

and directions of the curves C_l coincide with the system of normals to the surface thus $f_{l,i}\mu^{i}{}_{lk_1} = 0$ and (2.9) reduces to

$$\frac{1}{d_{kl}} = \frac{1}{\dfrac{\partial f_l}{dS_l}} \left\{ \frac{\partial f_{l,j}\lambda_{k_1}{}^{j}}{dS_l} - f_{l,i}\mu^{i}{}_{kl_1} + f_{l,i}\gamma_{lj}\lambda_{l_1}{}^{i}\lambda_{k_1}{}^{j} + f_{l,i}\lambda^{i}{}_{l_1,j}\lambda_{k_1}{}^{j} \right\}. \tag{3.4}$$

Further

$$\mu^i{}_{kl_1} = \Sigma\, \gamma_{krl}\lambda_{r_1}{}^i$$

and

$$\mu^i{}_{lk_1} = \Sigma\, \gamma_{lrk}\lambda_{r_1}{}^i. \tag{3.5}$$

Thus equation (2.8) can be put in terms of coefficients of rotation.

If we take the derivative of $\lambda_{h_1}{}^i\lambda_{k_1 i} = 0$ with respect to x^j and then multiply by $\lambda_{l_1}{}^j$ we have the relation

$$\gamma_{hkl_1} = -\gamma_{khl_1}. \tag{3.6}$$

Putting $h = k$ we get (3.7) $\gamma_{kkl_1} = 0$ in conformity with (3.3).

With the help of (3.5) we put (3.4) as

$$\frac{1}{d_{kl}} = \frac{1}{\dfrac{\partial f_l}{\partial S_l}}\left\{\frac{\partial f_{l,j}\lambda_{k_1}{}^j}{\partial S_l} + f_{l,i}\,\Sigma\,\gamma_{rkl}\lambda_{r_1}{}^i + f_{l,i'j}\lambda_{l_1}{}^i\,\lambda_{k_1}{}^j\right.$$

$$\left. + f_{l,i'}\lambda^i{}_{l_1,j}\lambda_{k_1}{}^j\right\}.$$

Thus if $\gamma_{rkl} = 0$ $(r = 1, 2, \ldots, n)$, $\lambda_{l_1}{}^i = 0$ and $f_{l,i}\lambda_{k_1}{}^i$ is invariant with respect to differentiation $\partial/\partial S_l$ the orthogonal ennuple of hypersurfaces is equidistant each hypersurface being so with respect to the congruence of curves not contained in it.

4. Distantial spread of one congruence of curves with respect to another congruence:—

We consider the n independent congruences of curves as obtained by the intersection of n independent families of hypersurfaces S_l,

$$f_l\left(x^1, x^2, \ldots, x^n, \frac{dx^1}{dS}, \frac{dx^2}{dS}, \ldots, \frac{dx^n}{dS}\right) = C_l$$

the curves C_l being the transversals of the hypersurfaces S_l.

Upon a two-dimensional surface $f_i = C_i\,(i = 1, 2, \ldots, n;\ i \neq k, l)$ there are ∞^1 curves C_l defined by the equations $f_k = C_k$ and ∞^1 curves C_k defined by the equations $f_l = C_l$.

Upon an arbitrary surface we consider these two sets of curves and take the logarithmic directional derivative of the distance measured along a curve of congruence C_l between the two neighbouring curves given by

$f_l = f_l^1, f_l = f_l^1 + f_l^0$ (where f_l^0 is of the order $4f_l^1$) of the congruence C_k. The limit of this derivative as $f_l^0 \to 0$ is the distantial spread of the curves C_k with respect to the curves C_l.

From (2.12) the distantial spread of the congruences of curves to one another can be put down as

$$\frac{1}{d_{kl}} = \frac{1}{\dfrac{\partial f_l}{\partial S_l}}\left[\frac{\partial f_{l,j}\lambda_{k_1}{}^j}{\partial S_l} + f_{l,i}(\mu^i{}_{lk_1} - \mu^i{}_{kl_1}) + f_{l,i'j}\lambda_{l_1}{}^i\ \lambda_{k_1}{}^j\right.$$

$$\left. + f_{l,i'}\lambda^i{}_{l_1,j}\lambda_{k_1}{}^j\right]$$

and

$$\frac{1}{d_{lk}} = \frac{1}{\dfrac{\partial f_k}{\partial S_k}}\left[\frac{\partial f_{k,j}\lambda_{l_1}{}^j}{\partial S_k} + f_{k,i}(\mu^i{}_{kl_1} - \mu^i{}_{lk_1}) + f_{k,i'j}\lambda_{k_1}{}^i\lambda_{l_1}{}^j\right.$$

$$\left. + f_{k,i'}\lambda_{k_1}{}^{i'}\lambda_{l_1}{}^j\right]. \qquad (4.1)$$

Thus

If the curves of each of two congruences are parallel with respect to one another, $\lambda_{l_1}{}^i$ and $\lambda_{k_1}{}^{i'}$ are null and the terms

$$\frac{\partial f_{l,j}\lambda_{k_1}{}^j}{\partial S_l}, \quad \frac{\partial f_{k,j}\lambda_{l_1}{}^j}{\partial S_k}$$

vanish then the curves of each congruence are equidistant with respect to the curves of the other.

Conversely if the first, third and fourth terms of both the brackets vanish and the curves of each congruence are equidistant with respect to the curves of another then their associate curvatures with respect to one another are identical.

Finally if the first, third and fourth terms of (4.1) vanish and the curves of each of the two congruences are equidistant with respect to another and the curves of one of the congruences are known to be parallel with respect

to another then the curves of latter congruence are also parallel with respect to the curves of first.

If the congruences form an orthogonal system, equations (4.1) simplify to

$$\frac{1}{d_{kl}} = \frac{1}{\dfrac{\partial f_l}{\partial S_l}} \left\{ \frac{\partial f_{l,j} \lambda_{k_1}{}^{j}}{\partial S_l} + f_{l,i} \Sigma \gamma_{rkl} \lambda_{r_1}{}^{i} + f_{l,i'j} \lambda_{l_1}{}^{i'} \lambda_{k_1}{}^{j} \right.$$

$$\left. + f_{l,i'} \lambda^{i}{}_{l_1,\ j} \lambda_{k_1}{}^{j} \right\}$$

$$\frac{1}{d_{kl}} = \frac{1}{\dfrac{\partial f_k}{\partial S_k}} \left\{ \frac{\partial f_{k,j} \lambda_{l_1}{}^{j}}{\partial S_k} + f_{k,i} \Sigma \gamma_{rlk} \lambda_{r_1}{}^{i} + f_{k,i'j} \lambda_{k_1}{}^{i'} \lambda_{l_1}{}^{j} \right.$$

$$\left. + f_{l,i'} \lambda^{i}{}_{k_1,j} \lambda_{l_1}{}^{j} \right\}. \tag{4.2}$$

Thus if

$$\frac{\partial f_{l,j} \lambda_{k_1}{}^{j}}{\partial S_l}, \quad \frac{\partial f_{k,j} \lambda_{l_1}{}^{j}}{\partial S_k}, \quad \lambda_{l_1}{}^{i'}, \quad \lambda_{k_1}{}^{i'}$$

are zero and the coefficients of rotation

$$\gamma_{rkl} = 0 \quad \text{for} \quad r = 1, 2, \ldots, n$$

then the curves of each of the congruences are equidistant with respect to another.

Conversely if

$$\frac{\partial f_{l,j} \lambda_{k_1}{}^{j}}{\partial S_l}, \quad \frac{\partial f_{k,j} \lambda_{l_1}{}^{j}}{\partial S_k}, \quad \lambda_{l_1}{}^{i}, \quad \lambda_{k_1}{}^{i}$$

are zero and the curves of each congruence are equidistant with respect to another, then the coefficients of rotation γ_{rkl} must be zero for all r.

Now

$$\lambda_{l_1}{}^{i_1} = \frac{dx'^{i}}{dS_l} = x,_{j'}{}^{i} \lambda_{l_1}{}^{j}$$

$$= \lambda^{i}{}_{m_1,j} \lambda_{l_1}{}^{j}$$

where m may stand for any number $1, 2, \ldots, n$.

Therefore,

$$\lambda_{l_1}{}^{i} = \mu^{i}{}_{m l_1}.$$

and

$$\mu^{i}{}_{ml_1} = \Sigma\, \gamma_{mrl}\lambda_{r_1}{}^{i}$$
$$= -\Sigma\, \gamma_{rml}\lambda_{r_1}{}^{i}.$$

Putting this value of $\lambda_{l_1}{}^{i}$ and $\lambda_{k_1}{}^{i}$ in (4.2) we have

$$\frac{1}{d_{kl}} = \frac{1}{\dfrac{\partial f_l}{\partial S_l}}\left[\frac{\partial f_{l,j}\lambda_{k_1}{}^{j}}{\partial S_l} + f_{l,i}\sum_r \gamma_{rkl}\lambda_{r_1}{}^{i} - f_{l,i'j}\sum_r \gamma_{rml}\lambda_{r_1}{}^{i}\lambda_{k_1}{}^{j}\right.$$
$$\left. - f_{l,i'}\left(\sum_r \gamma_{rml}\lambda_{r_1}{}^{i}\right), {}_j\lambda_{k_1}{}^{j}\right].$$

Hence we have, if

$$\gamma_{rkl} = 0 \quad \text{for} \quad r = 1, 2, \ldots, n$$

and

$$\frac{\partial f_{l,j}\lambda_{k_1}{}^{j}}{\partial S_l}, \quad \frac{\partial f_{k,j}\lambda_{l_1}{}^{j}}{\partial S_k}$$

are zero the curves of the orthogonal congruences are equidistant with respect to each other.

Conversely if the curves of two congruences are equidistant with respect to each other and

$$\frac{\partial f_{l,j}\lambda_{k_1}{}^{j}}{\partial S_l}, \quad \frac{\partial f_{k,j}\lambda_{l_1}{}^{j}}{\partial S_k}$$

are zero the coefficients of rotation γ_{rkl} must be zero for all r.

Section II

5. In the first section our findings in Finsler spaces were based on element of support and, therefore, on Euclidean connection.

In the present section we make a general approach by considering the Finsler space which is locally Minkowskian.

The metric function of n-dimensional Finsler space F_n is denoted by $F(x^i, X^i)$ where X^i is the vector attached to the point $P(x)$ of F_n. The function F is restricted by following assumptions:

(i) F is analytic in its $2n$ arguments $(x^1, x^2, \ldots, x^n; X^1, X^2, \ldots, X^n)$.

(ii) F is positive unless all the X^i vanish simultaneously.

(iii) It is positively homogeneous of the first degree in X^i.

(iv) The quadratic form $g_{ij}(x, X)\,\xi^i\xi^j > 0$ for $\xi^i \neq 0$

where

$$g_{ij}(x, X) = \tfrac{1}{2}\frac{\partial^2 F^2(x, X)}{\partial X^i \partial X^j}.$$

From assumption (iii) and by Euler's theorem on Homogeneous functions it follows:

$$\frac{\partial g_{ij}(x, X)}{\partial X^k} X^k = \frac{\partial g_{ij}(x, X)}{\partial X^h} X^j = 0 \tag{5.1}$$

$$g_{ij,k}(x, X)\, X^k = g_{ij,k}(x, X)\, X^j = 0. \tag{5.1 a}$$

In particular if $X^i = x'^i$ is contravariant component of the tangent vector then (5.1) takes the form

$$\frac{\partial g_{ij}(x, x')}{\partial x'^k} x'^k = \frac{\partial g_{ij}(x, x')}{\partial x'^h} x'^j = 0. \tag{5.2}$$

The co-variant derivative of a vector λ^i is given by

$$\lambda^i{}_{,k} = \frac{\partial \lambda^i}{\partial x^k} + P_{hk}{}^{*i}(x, X)\,\lambda^h \tag{5.3}$$

and the condition of parallelism is

$$\lambda^i{}_{,k} = 0.$$

In analogy to Riemannian space we define the associate curvature vector of λ^i with respect to X^k as its derived vector in the direction of X^k, that is

$$\lambda^i{}_{,k} X^k = \mu^i.$$

The measure of the associate curvature (angular spread) vector μ^i is given by the relation

$$\frac{1}{r^2} = g_{ij}(x, \mu)\,\mu^i\mu^j \tag{5.4}$$

and $1/r$ is called the associate curvature of λ^i with respect to curve C.

X^k are the contravariant components of the vector which is intrinsically attached to the point in question.

It is to be noted that in Riemannian space and locally Euclidean Finsler space the co-variant component μ_i of the associate curvature vector μ^i can be put as

$$\lambda_{i,k}\frac{dx^k}{dS} = \mu_i$$

whereas in this case on account of non-vanishing of $g_{ij,k}(x, X)$ it cannot be put in the above manner.

We call the vector

$$\lambda_{i,k}\frac{dx^k}{dS} = \mu_i$$

as the secondary associate curvature vector and the corresponding length given by

$$g^{ij}(x, \mu)\,\mu_i\mu_j = \frac{1}{r^2}$$

as the secondary associate curvature of the vector λ^i with respect to the curve C.

Obviously $g_{ij}(x, \mu)$ and $g^{ij}(x, \mu)$ are not the counterparts of each other. Corresponding to each associate curvature vector at a point of the curve we shall have the secondary curvature vector too.

As the contravariant components λ^i belong to a unit vector we have

$$g_{ij}(x, X)\,\lambda^i\lambda^j = 1$$

and the co-variant derivative with respect to x^k gives

$$g_{ij,k}(x, X)\,\lambda^i\lambda^j + 2g_{ij}(x, X)\,\lambda^i{}_{,k}\lambda^j = 0$$

or

$$g_{ij,k}(x, X)\,\lambda^i\lambda^j x'^k + 2g_{ij}(x, X)\,\lambda^i{}_{,k}\lambda^j x'^k = 0. \qquad (5.5)$$

Thus we observe that unlike Finsler manifolds with Euclidean connection here the vector μ^i is not always perpendicular to λ^i; it is perpendicular only when first term of (5.5) vanishes, *i.e.*, when X^i are replaced by λ^i in $g_{ij}(x, X)$ or $X^i \equiv x'^i$.

If n linearly independent congruences of curves C_k $(k = 1, 2, \ldots, n)$ with tangent vector

$$\lambda_{k_1}{}^i = \frac{dx^i}{dS_k}$$

are considered then the associate curvature vectors of the vectors $\lambda_{k_1}{}^i$ with respect to curves C_l $(k, l = 1, 2, \ldots, n,\ k \neq l)$ are given by

$$\mu^j{}_{kl_1} = \lambda^j{}_{k_1,i}\lambda_{l_1}{}^i. \tag{5.6}$$

This is called the angular spread vector or the associate curvature vector of the curves C_k with respect to C_l and its length

$$\frac{1}{r_{kl}{}^2} = g_{ij}(x, \mu_k)\,\mu^i{}_{kl_1}\mu^j{}_{kl_1}$$

is called the associate curvature of the curves C_k with respect to C_l.

Here again we notice that $\mu^i{}_{kl_1}$ are not necessarily perpendicular to $\lambda_{k_1}{}^i$; they will be so only when

$$g_{ij,h}(x, X)\,\lambda_{k_1}{}^i\lambda_{k_1}{}^j\lambda_{l_1}{}^h = 0,\ \textit{i.e.},\ X^i = \lambda_{k_1}{}^i \text{ or } X^i = \lambda_{l_1}{}^i. \tag{5.7}$$

If F_n is a subspace embedded in a Finsler space F_m, $(m > n)$ the vectors in F_m are specified by λ^i whose contravariant components in F_n are ξ^α thus

$$\lambda^i = X_\alpha{}^i\xi^\alpha \qquad \left\{ \begin{array}{c} i, j, k = 1, 2, \ldots, n \\ \alpha, \beta, \gamma = 1, 2, \ldots, n \\ x^i = x^i(u^1, u^2, \ldots, u^n) \end{array} \right\}. \tag{5.8}$$

Its ordinary differentiation gives

$$\frac{d\lambda^i}{dS} = X_\alpha{}^i\frac{d\xi^\alpha}{dS} + \frac{\partial^2 x^i}{\partial u^\alpha \partial u^\beta}\,\xi^\alpha\frac{du^\beta}{dS}. \tag{5.9}$$

The associate curvature vector of λ^i are denoted by μ then

$$\mu^i = \frac{dx^j}{dS}\,\lambda^i{}_{,j}. \tag{5.10}$$

On account of (5.8) and (5.9) it takes the following form

$$\mu^i = \frac{d\xi^\alpha}{dS}\,X_\alpha{}^i + \xi^\alpha\frac{du^\beta}{dS}\left(\frac{\partial^2 x^i}{\partial u^\alpha \partial u^\beta} + P_{hk}{}^{*i}X_\alpha{}^h X_\beta{}^k\right). \tag{5.11}$$

Since

$$P^*{}_{\alpha\beta,\gamma}(u, u') = g_{ij}(x, x')\,X_\gamma{}^j\left(\frac{\partial^2 x^i}{\partial u^\alpha \partial u^\beta} + P_{hk}{}^{*i}(x, x')\,X_\alpha{}^h X_\beta{}^k\right).$$

We have

$$g_{ij}(x, x')\,X_\gamma{}^i\mu^j = g_{\alpha\gamma}\xi^\alpha{}_{,\beta}\frac{du^\beta}{dS} = g_{\alpha\gamma}(u, u')\,\eta^\alpha \tag{5.12}$$

where we have put

$$\xi^{\alpha}{}_{,\beta}\frac{du^{\beta}}{dS}=\eta^{\alpha}$$

which is the associate curvature vector of ξ^{α} with respect to the same curve C.

Thus the relation (5.12) shows that the associate curvature vector of vectors in subspace and the embedding space with respect to same curve is not necessarily the same.

The associate curvature of the vector λ^{i} with respect to curve C is essentially its measure of the deviation from parallelism with respect to curve C.

6. *Equidistance of families of hypersurfaces with respect to congruences of curves.*—Let n independent families of hypersurfaces S_l be defined in F_n by the equations $f_l(x^1, x^2, \ldots, x^n, x'^1, \ldots, x'^n) = C_l$ $(l = 1, 2, \ldots, n)$.

The n linearly independent congruences of curves which are the curves of intersection of these hypersurfaces are denoted by C_k $(k = 1, 2, \ldots, n)$ and their unit tangent vectors are

$$\lambda_{k_i}{}^{i}=\frac{dx^{i}}{dS_k}.$$

The hypersurfaces S_l of the family $f_l = C_l$ contain $(n-1)$ congruences of curves C_k $(k \neq l)$ and the congruence C_l is their transversal.

We define the distantial spread of the hypersurfaces S_l with respect to the curves C_l measured along C_k in the same way as we did in Section I.

Thus

$$\frac{1}{d_{kl}}=\text{Lt.}_{f_l^0\to 0}\frac{\partial \log d_l}{\partial S_k}\qquad (k\neq l)$$

or

$$\frac{1}{d_{kl}}=-\frac{\partial \log\left(\frac{\partial f_l}{\partial S_l}\right)}{\partial S_k}. \tag{6.1}$$

If $1/d_{kl}=0$ then $\log \partial f_l/\partial S_l$ is constant and $S_l = F(f_l)$ is the common directed arc measured from a fixed hypersurface S_k of all the curves C_l.

Conversely when $1/d_{kl}$ the distantial spread of hypersurfaces S_l with respect to curves C_l in the directions of the curves C_k $(k \neq l)$ is zero at all points then each pair of hypersurfaces cut equal segments on transversals.

Now

$$f_l(x^1, x^2, \ldots, x^n, x'^1, \ldots, x'^n) = C_l.$$

and

$$\frac{\partial f_l}{\partial S_l} = \frac{\partial f_l}{\partial x^i}\frac{dx^i}{dS_l} + \frac{\partial f_l}{\partial x'^i}\frac{dx'^i}{dS_l}$$
$$= f_{l,i}\lambda_{l_1}{}^i + f_{l,i'}\lambda_{l_1}{}^i$$

where we have put

$$\lambda_{l_1}{}^{i'} = \frac{dx'^i}{dS_l}. \tag{6·2}$$

Therefore

$$\frac{1}{d_{kl}} = -\frac{1}{\dfrac{\partial f_l}{\partial S_l}}(f_{l,i}\lambda_{l_1}{}^i + f_{l,i'}\lambda_{l_1}{}^i)_{,j}\lambda_{k_1}{}^j$$
$$= -\frac{1}{\dfrac{\partial f_l}{\partial S_l}}(f_{l,ij}\lambda_{l_1}{}^i + f_{l,i}\lambda^i{}_{l_1,j} + f_{l,i'j}\lambda_{l_1}{}^i + f_{l,i'}\lambda^i{}_{l_1,j})\lambda_{k_1}{}^j. \tag{6.3}$$

Also

$$f_{l,ij}\lambda_{l_1}{}^i\lambda_{k_1}{}^j = \frac{\partial f_{l,j}\lambda_{k_1}{}^j}{\partial S_l} - f_{l,j}\lambda^j{}_{k_1,i}\lambda_{l_1}{}^i.$$

Substituting this value of $f_{l,ij}\lambda_{l_1}{}^i\lambda_{k_1}{}^j$ in (6.3) and taking into account (5.6) we have

$$\frac{1}{d_{kl}} = \frac{1}{\dfrac{\partial f_l}{\partial S_l}}\Big[f_{l,i}(\mu^i{}_{kl_1} - \mu^i{}_{lk_1}) - \frac{\partial}{\partial S_l}(f_{l,j}\lambda_{k_1}{}^j)$$
$$- f_{l,i'j}\lambda_{l_1}{}^{i'}\lambda_{k_1}{}^j - f_{l,i'}\lambda^i{}_{l_1,j}\lambda_{k_1}{}^j\Big]. \tag{6.4}$$

From (6.4) we obtain the following theorems:

THEOREM 1.—*The hypersurfaces are equidistantial with respect to the curves C_k, if the difference vector of the associate curvatures of curves C_l with respect to C_k and curves C_k with respect to C_l is null and the last three terms reduce to zero.*

In particular if the congruence of curves C_l are geodesics, $\lambda_{l_1}{}^{i'}$ will be zero.

THEOREM 2.—*Similarly if the unit tangent vectors* $\lambda_{k_1}{}^i$ *and* $\lambda_{l_1}{}^i$ *are parallel with respect to the curves* C_l *and* C_k *respectively and the last three terms are zero the hypersurfaces* S_l *will be equidistant with respect to curves* C_k.

Now

$$\lambda_{l_1}{}^i = x'^i{}_{,j}\lambda_{l_1}{}^j$$
$$= \lambda^i{}_{m_1,j}\lambda_{l_1}{}^j = \mu^i{}_{ml_1}.$$

Thus $\lambda_{l_1}{}^i$ is actually the associate curvature vector with one of the superscript suppressed meaning thereby that it stands for the associate curvature of all the curves of the congruences C_m $(m = 1, 2, \ldots, n)$.

Therefore

$$\frac{1}{d_{kl}} = \frac{1}{\dfrac{\partial f_l}{\partial S_l}}\Big[f_{l,i}(\mu^i{}_{kl_1} - \mu^i{}_{lk_1}) - \frac{\partial}{\partial S_l}(f_{l,j}\lambda_{k_1}{}^j)$$

$$- f_{l,i'j}\mu^i{}_{ml_1}\lambda_{k_1}{}^j - f_{l,i'}\mu^i{}_{ml_1,j}\lambda_{k_1}{}^j \Big]. \tag{6.5}$$

Thus we have

THEOREM 3.—*The hypersurfaces* S_l *are equidistant with respect to the curves* C_k *if the associate curvature vectors of all the curves of the congruence with respect to the fixed congruence* C_l *are zero, the associate curvature vectors of* C_l *with respect to* C_k *are zero and the sum* $f_{l,j}\lambda_{k_1}{}^j$ *is independent of* s_l.

7. We choose an orthogonal ennuple of hypersurfaces in F_n such that if

$$\lambda_{k_1}{}^i = \frac{dx^i}{dS_l}, \quad \lambda_{l_1}{}^j = \frac{dx^j}{dS_l}$$

be the contravariant components of the unit tangent vectors of the transversals C_k and C_l of the family of hypersurfaces $f_k = C_k$, $f_l = C_l$ then we have the relations

$$g_{ij}(x, \lambda_{k_1})\lambda_{k_1}{}^i\lambda_{l_1}{}^j = \delta_l{}^k = \lambda_{k_1 j}\lambda_{l_1}{}^j$$
$$g_{ij}(x, \lambda_{l_1})\lambda_{l_1}{}^i\lambda_{k_1}{}^j = \delta_k{}^l = \lambda_{l_1 j}\lambda_{k_1}{}^j. \tag{7.1}$$

It is to be noted that $\delta_l{}^k \neq \delta_k{}^l$ in general, though of course $\delta_l{}^k$ and $\delta_k{}^l$ are both zero or one according as $k \neq l$ or $k = l$.

The projection of the derived vector of λ_{h_l} in the direction of λ_{l_l} on λ_{k_l} is given by

$$\lambda^i{}_{h_l,j}\lambda_{k_l i}\lambda_{l_l}{}^j \tag{7.2}$$

we put it as γ_{hkl} and call it Ricci's coefficient of rotation.

Since

$$\lambda^i{}_{h_l,j}\lambda_{k_l i} \neq \lambda_{h_l i,j}\lambda_{k_l}{}^i$$

the coefficient of rotation so defined is not anti-symmetric in the first two indices.

We call the invariant defined by

$$\lambda_{h_l i,j}\lambda_{l_l}{}^j\lambda_{k_l}{}^i = \gamma_{hkl} \tag{7.3}$$

as the relative Ricci's coefficient of rotation.

Taking the co-variant derivative of the relation (7.1) with respect to x^m, multiplying it by $\lambda_{l_l}{}^m$ we have

$$\begin{aligned}&(\lambda_{h_l j,m}\lambda_{k_l}{}^j + \lambda_{h_l j}\lambda^j{}_{k_l,m})\,\lambda_{l_l}{}^m = 0\\ &(\lambda^j{}_{h_l,m}\lambda_{k_l j} + \lambda_{h_l}{}^j\lambda_{k_l j,m})\,\lambda_{l_l}{}^m = 0.\end{aligned} \tag{7.4}$$

In view of (7.2) and (7.3) we have

$$\begin{aligned}&\gamma_{hkl} + \gamma_{khl} = 0\\ &\gamma_{hkl} + \gamma_{khl} = 0\end{aligned} \tag{7.5}$$

This shows that the relative coefficient of rotation and coefficient of rotation are connected by a reciprocal relation.

From (7.2) and (7.3) we have relations for associate and secondary associate curvature vector, thus,

$$\begin{aligned}&\lambda^i{}_{h_l,j}\lambda_{l_l}{}^j = \sum_k \gamma_{hkl}\lambda_{k_l}{}^i = \mu^i{}_{hl_l}\\ &\lambda_{h_l i,j}\lambda_{l_l}{}^j = \sum_k \gamma_{hkl}\lambda_{k_l i} = \mu_{hl_l i}.\end{aligned} \tag{7.6}$$

We may remark here that if λ's are constant multiples of each other then in view of condition (iii), the distinction between two types of associate curvatures and Ricci's coefficient of rotation will vanish.

The derived vector of λ_{h_l} in its own direction is called the first curvature vector and is denoted by

$$\lambda^i{}_{h_1,j}\lambda_{h_1}{}^j = \sum_k \gamma_{hkh}\lambda_{k_1}{}^i = \mu_{h_1}{}^i$$

$$\lambda_{h_1 i,j}\lambda_{h_1}{}^j = \sum_k \gamma_{hkh}\lambda_{k_1 i} = \mu_{h_1 i}. \tag{7.7}$$

Applying (7.6) to (6.5) we have

$$\frac{1}{d_{kl}} = \frac{1}{\dfrac{\partial f_l}{\partial S_l}}\Big[f_{l,i}\Big(\sum_h \gamma_{khl}\lambda_{h_1}{}^i - \sum_h \gamma_{lhk}\lambda_{h_1}{}^i\Big) - \frac{\partial}{\partial S_l}(f_{l,j}\lambda_{k_1}{}^j)$$

$$- f_{l,i'j}\sum_h \gamma_{mhl}\lambda_{h_1}{}^i\lambda_{k_1}{}^j - f_{l,i'}\Big(\sum_h \gamma_{mhl}\lambda_{h_1}{}^i\Big)_{,j}\lambda_{k_1}{}^j\Big]. \tag{7.8}$$

Hence we have

THEOREM 4.—*If for an orthogonal ennuple of hypersurfaces the Ricci's coefficients of rotation* $\gamma_{hkl_1} = 0$ $(h, k, l = 1, 2, \ldots, n)$ and $\partial/S_l(f_{l,j}\lambda_{k_1}{}^j)$ *is also zero then the family of hypersurfaces* $f_l = C_l$ *must be equidistant with respect to the family* $f_k = C_k$.

On account of (7.5) the relation (7.8) can also be put as

$$\frac{1}{d_{kl}} = \frac{1}{\dfrac{\partial f_l}{\partial S_l}}\Big[f_{l,i}\Big(\sum_h \gamma_{hlk}\gamma_{h_1}{}^i - \sum_h \lambda_{hkl}\lambda_{h_1}{}^i\Big) - \frac{\partial}{\partial S_l}(f_{l,j}\lambda_{k_1}{}^j)$$

$$+ f_{l,i'j}\sum_h \gamma_{hml}\lambda_{h_1}{}^i\lambda_{k_1}{}^j - f_{l,i'}\Big(\sum_h \gamma_{hml}\lambda_{h_1}{}^i\Big)_{,j}\lambda_{k_1}{}^j\Big].$$

Hence

THEOREM 5.—*The family of hypersurfaces* $f_l = C_l$ *will be equidistant with respect to* $f_k = C_k$ *if relative coefficients of rotation* γ_{hkl} *are zero and* $\partial/\partial S_l(f_{l,j}\lambda_{k_1}{}^j)$ *is zero.*

8. We define the distantial spread of the curves of the congruences on the same lines as in Section I, thus the distantial spread of the curves of the congruence C_k with respect to the curves of the congruence C_l can be put as

$$\frac{1}{d_{kl}} = \frac{1}{\dfrac{\partial f_l}{\partial S_l}}\Big[f_{l,i}(\mu^i{}_{lk_1} - \mu^i{}_{kl_1}) - \frac{\partial}{\partial S_l}(f_{l,j}\lambda_{k_1}{}^j)$$

$$- f_{l,i'j}\mu^i{}_{ml_1}\lambda_{k_1}{}^j - f_{l,i'}\mu^i{}_{ml_1,j}\lambda_{k_1}{}^j\Big]. \tag{8.1}$$

Similarly we have

$$\frac{1}{d_{kl}} = \frac{1}{\dfrac{\partial f_k}{\partial S_k}}\Big[f_{k,i}(\mu^i{}_{lk_1} - \mu^i{}_{kl_1}) - \frac{\partial}{\partial S_k}(f_{k,j}\lambda_{l_1}{}^j)$$

$$- f_{k,i'j}\mu^i{}_{mk_1}\lambda_{l_1}{}^j - f_{k,i'}\mu^i{}_{mk_1,j}\lambda_{k_1}{}^j\Big]. \tag{8.2}$$

The distantial spread of congruence of curves C_k with respect to the congruences C_l will be zero if $1/d_{kl}$ is zero.

Thus we have

THEOREM 6.—*If the curves of all the congruences are parallel with respect to the curves of congruences C_l and curves of congruence C_l are parallel with respect to C_k and $f_{l,j}\lambda_{k_1}{}^j$ is invariant with respect to the differentiation $\partial/\partial S_l$ then the curves of congruence C_k are equidistant with respect to the curves of congruence C_l.*

As (8.1) is equivalent to the following equation

$$\frac{1}{d_{kl}} = \frac{1}{\dfrac{\partial f_l}{\partial S_l}}\Big[f_{l,i}(\mu^i{}_{kl_1} - \mu^i{}_{lk_1}) - \frac{\partial}{\partial S_l}(f_{l,j}\lambda_{k_1}{}^j)$$

$$- f_{l,i'j}\lambda_{l_1}{}^{i'}\lambda_{k_1}{}^j - f_{l,i'}\lambda^i{}_{l_1,j}\lambda_{k_1}{}^j\Big] \tag{8.3}$$

We have

THEOREM 7.—*If the curves of two congruences C_k, C_l are parallel with respect to each other, $\partial/\partial S_l\,(f_{l,j}\lambda_{k_1}{}^j)$ is zero and the vector $\lambda_{l_1}{}^{i'}$ is null then the curves of congruence C_k are equidistant with respect to the curves of congruence C_l.*

Considering (8.1) and (8.2) together we have

THEOREM 8.—*If the curves of two congruences C_k and C_l are parallel with respect to each other $\partial/\partial S_l\,(f_{l,j}\lambda_{k_1}{}^j)$, $\partial/\partial S_k\,(f_{k,j}\lambda_{l_1}{}^j)$ is zero and the vectors $\lambda_{l_1}{}^{i'}$, $\lambda_{k_1}{}^{i'}$ are null then both the congruences are equidistant with respect to each other.*

REFERENCES

1. Graustein .. "Parallelism and equidistance in classical differential geometry," *Trans. Ame. Math. Soc.*, 1932, **34**, 557-93.
2. Cartan, E. .. "Le espaces de Finsler," *Actualities* 79, 1934, Paris.
3. Peters, R. M. .. "Parallelism and equidistance in Riemannian geometry," *Ame. Journ. Maths.*, 1935, **57**, 103-11.
4. ———— .. "Parallelism and equidistance of congruence of curves of orthogonal ennuples," *Ibid.*, 1937, **59**, 564-74.
5. Kawaguchi, A. .. "On the theory of non-linear connections—I," *Tensor New Series*, 1952, **12**, 123-42.
6. ———— .. "On the theory of non-linear connections—II," *Ibid.*, 1956, **6**, 165-99.
7. Rund, H. .. "On the analytical properties of curvature tensor," *Math. Ann.*, 1954, **127**, 82-104.
8. ———— .. "Hypersurfaces of a Finsler space," *Can. Journ. of Maths.*, 1955, **8**, 487-503.

ON THE DECOMPOSITION OF THE FEYNMAN PROPAGATOR

BY ALLADI RAMAKRISHNAN,* F.A.SC.

(University of Bern, Switzerland)

T. K. RADHA‡ AND R. THUNGA

(University of Madras, India)

Received July 20, 1960

ABSTRACT

The Feynman propagator, in momentum representation, is a four-dimensional transform over space and time variables. If the space and time integrations are performed separately, the propagator can be decomposed into two parts, one corresponding to positive and the other to negative energy intermediate state. By the use of this decomposed propagator, the relative contributions of the positive and negative energy intermediate states to the matrix element can be estimated. For example in Compton scattering it leads to the apparently paradoxical result that in the "non-relativistic approximation" it is only the negative energy intermediate state that contributes to the matrix element.

INTRODUCTION

IT is well recognised that one of the great advances in quantum electrodynamics since the Dirac theory of the electron is the Feynman formulation which is characterised essentially by two features: (i) Even when we include pair creation and annihilation of particles the vertices of interaction in perturbation theory can be so ordered in the Feynman sense such that the entire process can be represented through Feynman graphs of single particles thus obviating the use of field theoretic methods and (ii) the perturbation expansions are "inherently four-dimensional" and the covariance of the equations is apparent at every stage of the calculations, the integrations over space and time variables being performed together.

---

* Permanent address: University of Madras, India. The above work was done during the author's stay at the Department of Theoretical Physics, University of Bern, on leave of absence from the University of Madras.

‡ Atomic Energy Commission Junior Research Fellow.

It has been pointed out by one of the authors (A. R.) that a better understanding of the virtual processes is possible if the space integration is performed first and the time integration subsequently in the " old-fashioned " manner even in the Feynman formulation. It is this method which gives a clearer picture of the contributions due to the different types of virtual processes. It leads to the splitting of the Feynman propagator and while not affecting the elegance of the inherently relativistic approach, reveals the structure of the Feynman propagator in a manner which facilitates the computation of the relative contributions from transitions to positive and negative energy intermediate states. In particular, calculations lead to the apparently paradoxical result that the negative energy states do contribute even if the electron in Compton scattering is non-relativistic. It is conventionally accepted that when the initial particles are non-relativistic, the energy denominators become large for negative energy states and therefore the contribution in such cases can be neglected. This assumption may lead to erroneous results since the numerators may also become large and this can only be studied by the use of the decomposed propagator.[1]

Decomposition of the Feynman Propagator

In the Feynman picture since a negative energy electron travels back in time, the positive and negative energy parts of the intermediate state can be separated by splitting the time integration in the perturbation expansion (*i.e.*, from $t = -\infty$ to $t = +\infty$) into two parts corresponding to the ranges 0 to $+\infty$ with energy $+E$ and $-\infty$ to 0 with energy $-E$ respectively. The integration over space variables alone in a perturbation expansion say for a process in which an electron of momentum $\vec{p}$ absorbs a photon of momentum $\vec{q}$, would amount to picking out from the kernel, terms corresponding to momentum $\vec{p} + \vec{q}$ and energy E equal to

$$\pm E_{p+q} = \pm \sqrt{\left(\vec{p} + \vec{q}\right)^2 + m^2}.$$

[1] The paradoxical result that the negative energy states should contribute even in the non-relativistic case seems to have been well recognized on the ground that the operator γ_μ connects the positive and negative energy states. What we wish to emphasise here is that the relative contributions can be studied by decomposing the Feynman propagator the energy denominators in this case being naturally different from the field theoretic case. This is so because the definition of the intermediate states in field theory refers to systems of electrons, positrons and photons while in the Feynman formalism it relates only to the electron.

If we now perform the time integrations separately corresponding to $+ E_{p+q}$ and $- E_{p+q}$ we have, for the Feynman propagator in momentum representation,[2]

$$\frac{1}{\not p + \not q - m} = \frac{1}{2}\left[\frac{\overset{+}{\not P} + m}{\left(E_{\vec{p}+\vec{q}}\right)\left\{E_{\vec{p}} + E_{\vec{q}} - E_{\vec{p}+\vec{q}}\right\}} - \frac{\bar{\not P} + m}{\left(E_{\vec{p}+\vec{q}}\right)\left\{E_{\vec{p}} + E_{\vec{q}} + E_{\vec{p}+\vec{q}}\right\}}\right] \tag{1}$$

where $P = p + q$ and $\overset{+}{\not p}$ is the Feynman four vector with energy $+ E_{\vec{p}+\vec{q}}$ and $\bar{\not P}$ has the fourth component equal to $- E_{\vec{p}+\vec{q}}$.

We shall now make use of the above expression for the propagator and calculate the cross-sections for Compton scattering taking into account intermediate states of positive energy only, forbidding intermediate states of negative energy and *vice-versa.*

The matrix element representing the scattering of an incident photon of momentum q_1 by an electron (at rest) to momentum q_2, the electron having a momentum p_2, is obtained by considering the two possibilities (1) the photon q_1 being absorbed and q_2 being emitted subsequently in the Feynman sense and (2) q_2 being emitted and q_1 absorbed subsequently.

The propagators for the two cases are given by

$$\frac{1}{\not p_1 + \not q_1 - m} = \frac{1}{2}\left[\frac{\overset{+}{\not P}_1 + m}{\left(E_{\vec{p}_1+\vec{q}_1}\right)\left\{E_{\vec{p}_1} + E_{\vec{q}_1} - E_{\vec{p}_1+\vec{q}_1}\right\}} - \frac{\bar{\not P}_1 + m}{E_{\vec{p}_1+\vec{q}_1}\left\{E_{\vec{p}_1} + E_{\vec{q}_1} + E_{\vec{p}_1+\vec{q}_1}\right\}}\right] \tag{2}$$

where $\not P_1$ has energy component $E_{\vec{p}_1+\vec{q}_1}$ and

---

[2] Throughout this paper, we work in natural units, *i.e.*, $c = 1$, $\hbar = 1$ and use the conventional Feynman notation: If p denotes the four vector with components p_x, p_y, p_z, $E_{\vec{p}}\left(\vec{p}, E_{\vec{p}}\right)$ then the Feynman four vector $\not p = p_\mu \gamma_\mu = E_{\vec{p}}\gamma_t - \vec{p}.\vec{\gamma}$, where γ's are the usual Dirac matrices and $\not p \not q = E_p \omega - \vec{\omega}.\vec{p}$, where q is another four vector with components $\left(\omega, \vec{\omega}\right)$.

$$\frac{1}{\not p_1 - \not q_2 - m} = \frac{1}{2}\left[\frac{\overset{+}{\not p}_2 + m}{\left(E_{\vec{p}_1-\vec{q}_2}\right)\left\{E_{\vec{p}_1} - E_{\vec{q}_2} - E_{\vec{p}_1-\vec{q}_2}\right\}} - \frac{\overline{\not p}_2 + m}{\left(E_{\vec{p}_1-\vec{q}_2}\right)\left\{E_{\vec{p}_1} - E_{\vec{q}_2} + E_{\vec{p}_1-\vec{q}_2}\right\}}\right] \tag{3}$$

where $\not p_2$ has energy component $E_{\vec{p}_1-\vec{q}_2}$.

The cross-sections for the entire process taking the effect of positive energy alone ignoring the negative energy part in the intermediate state can be calculated by using the sum of the first terms of (2) and (3) as the propagator. Thus the matrix element after substituting for $\overset{+}{\not p}_1$, etc., is

$$M^{(+)} = \frac{(-i)}{2}(4\pi e^2)\,\bar{u}_2\left[\not\varepsilon_2 \frac{\gamma_t\sqrt{\omega_1^2+m^2} - \gamma_x\omega_1 + m}{\sqrt{\omega_1^2+m^2}\{m+\omega_1-\sqrt{\omega_1^2+m^2}\}}\not\varepsilon_1 + \not\varepsilon_1 \frac{\gamma_t\sqrt{\omega_2^2+m^2}+\gamma_x\omega_2\cos\theta+\gamma_y\omega_2\sin\theta+m}{\sqrt{\omega_2^2+m^2}\{m-\omega_2-\sqrt{\omega_2^2+m^2}\}}\not\varepsilon_2\right]u_1. \tag{4}$$

$$M^{(-)} = \frac{+i}{2}(4\pi e^2)\,\bar{u}_2\left[\not\varepsilon_2 \frac{-\gamma_t\sqrt{\omega_1^2+m^2} - \gamma_x\omega_1 + m}{\sqrt{\omega_1^2+m^2}\{m+\omega_1+\sqrt{\omega_1^2+m^2}\}}\not\varepsilon_1 + \not\varepsilon_1 \frac{-\gamma_t\sqrt{\omega_2^2+m^2}+\gamma_x\omega_2\cos\theta+\gamma_y\omega_2\sin\theta+m}{\sqrt{\omega_2^2+m^2}\{m-\omega_2+\sqrt{\omega_2^2+m^2}\}}\not\varepsilon_2\right]u_1 \tag{5}$$

Taking the incoming photon to be along the x direction we have for polarisation

(A) $\not\varepsilon_1 = \gamma_z$ or (B) $\not\varepsilon_1 = \gamma_y$

and for the outgoing photon

(A′) $\not\varepsilon_2 = \gamma_z$ or (B′) $\not\varepsilon_2 = \gamma_y\cos\theta - \gamma_x\sin\theta$.

Thus the matrix elements $M^{(+)}$ and $M^{(-)}$ for various polarisation combinations are given by

$$M^{(+)}(\text{AB′ or BA′}) = \frac{1}{\sqrt{F_1F_2}}\frac{(-i4\pi e^2)}{2}\left[\frac{F_1F_2\{i\sqrt{\omega_1^2+m^2}-im\}e^{i\theta}+i\omega_1F_1p_{2+}e^{i\theta}}{\sqrt{\omega_1^2+m^2}\{m+\omega_1-\sqrt{\omega_1^2+m^2}\}} + \frac{F_1F_2\{-i\sqrt{\omega_2^2+m^2}+im\}e^{i\theta}+i\omega_2F_1p_{2+}}{\sqrt{\omega_2^2+m^2}\{m-\omega_2-\sqrt{\omega_2^2+m^2}\}}\right] \tag{6}$$

where $p_{2+} = p_{2x} + ip_{2y}$

and

$$M^{(-)}(AB' \text{ or } BA')$$

$$= \frac{1}{\sqrt{F_1F_2}}\left(\frac{-i4\pi e^2}{2}\right)\left[\frac{F_1F_2\,(i\sqrt{\omega_1^2+m^2}+im)\,e^{i\theta}-i\omega_1F_1p_{2+}e^{i\theta}}{\sqrt{\omega_1^2+m^2}\,\{m+\omega_1+\sqrt{\omega_1^2+m^2}\}}\right.$$

$$\left.+\frac{F_1F_2\,\{-i\sqrt{\omega_2^2+m^2}-im\}\,e^{i\theta}-i\omega_2F_1p_{2+}}{\sqrt{\omega_2^2+m^2}\,\{m-\omega_2+\sqrt{\omega_2^2+m^2}\}}\right]. \tag{7}$$

$$M^{(+)}(AA')$$

$$= \frac{1}{\sqrt{F_1F_2}}\,\frac{(-i4\pi e^2)}{2}\left[\frac{F_1F_2\,\{\sqrt{\omega_1^2+m^2}-m\}-\omega_1F_1p_{2-}}{\sqrt{\omega_1^2+m^2}\,\{m+\omega_1-\sqrt{\omega_1^2+m^2}\}}\right.$$

$$\left.+\frac{F_1F_2\,\{\sqrt{\omega_2^2+m^2}-m\}+\omega_2F_1p_{2-}e^{i\theta}}{\sqrt{\omega_2^2+m^2}\,\{m-\omega_2-\sqrt{\omega_2^2+m^2}\}}\right]. \tag{8}$$

$$M^{(-)}(AA')$$

$$= \frac{1}{\sqrt{F_1F_2}}\left(\frac{-i4\pi e^2}{2}\right)\left[\frac{F_1F_2\,\{\sqrt{\omega_1^2+m^2}+m\}+\omega_1F_1p_{2-}}{\sqrt{\omega_1^2+m^2}\,\{m+\omega_1+\sqrt{\omega_1^2+m^2}\}}\right.$$

$$\left.+\frac{F_1F_2\,\{\sqrt{\omega_2^2+m^2}+m\}-\omega_2F_1p_{2-}e^{i\theta}}{\sqrt{\omega_2^2+m^2}\,\{m-\omega_2+\sqrt{\omega_2^2+m^2}\}}\right]. \tag{9}$$

$$M^{(+)}(BB')$$

$$= \frac{1}{\sqrt{F_1F_2}}\,\frac{(-i4\pi e^2)}{2}\left[\frac{F_1F_2\,\{\sqrt{\omega_1^2+m^2}e^{-i\theta}-me^{-i\theta}\}-\omega_1F_1p_{2-}e^{i\theta}}{\sqrt{\omega_1^2+m^2}\,\{m+\omega_1-\sqrt{\omega_1^2+m^2}\}}\right.$$

$$\left.+\frac{F_1F_2\,\{\sqrt{\omega_2^2+m^2}e^{i\theta}-me^{i\theta}\}+\omega_2F_1p_{2-}}{\sqrt{\omega_2^2+m^2}\,\{m-\omega_2-\sqrt{\omega_2^2+m^2}\}}\right] \tag{10}$$

and

$$M^{(-)}(BB')$$

$$= \frac{1}{\sqrt{F_1F_2}}\,\frac{(-i4\pi e^2)}{2}\left[\frac{F_1F_2\,\{\sqrt{\omega_1^2+m^2}e^{-i\theta}+me^{-i\theta}\}+\omega_1F_1p_{2-}e^{i\theta}}{\sqrt{\omega_1^2+m^2}\,\{m+\omega_1+\sqrt{\omega_1^2+m^2}\}}\right.$$

$$\left.+\frac{F_1F_2\,\{\sqrt{\omega_2^2+m^2}e^{i\theta}+me^{i\theta}\}-\omega_2F_1p_{2-}}{\sqrt{\omega_2^2+m^2}\,\{m-\omega_2+\sqrt{\omega_2^2+m^2}\}}\right] \tag{11}$$

where

$$F_2 = E_2 + m, \quad F_1 = E_1 + m.$$

For any one of the polarization cases considered above, we sum over the initial spin states of the electron and average over the final spin states to obtain the cross-section. We shall now list $|M|^2$ for the various combinations of polarization.

$$|M^{(+)}(\mathrm{AB'\ or\ BA'})|^2$$

$$= \frac{1}{4F_1F_2}(4\pi e^2)^2 \left[\frac{F_1^2F_2^2(\omega_1^2 + 2m^2 - 2m\sqrt{\omega_1^2+m^2}) + F_1^2\omega_1^2\vec{p}_2^{\,2} + (\sqrt{\omega_1^2+m^2}-m) \times 2F_1^2F_2\omega_1 p_{2x}}{(\omega_1^2+m^2)\{2m^2+2\omega_1^2+2m\omega_1 - 2(m+\omega_1)\sqrt{\omega_1^2+m^2}\}} \right.$$

$$+ \frac{F_1^2F_2^2(\omega_2^2+2m^2-2m\sqrt{\omega_2^2+m^2}) + F_1^2\omega_2^2\vec{p}_2^{\,2} - 2F_1^2F_2\omega_2 \times (p_{2x}\cos\theta + p_{2y}\sin\theta)(\sqrt{\omega_2^2+m^2}-m)}{(\omega_2^2+m^2)\{2m^2+2\omega_2^2-2m\omega_2-2(m-\omega_2)\sqrt{\omega_2^2+m^2}\}}$$

$$\left. + \frac{-2F_1^2F_2^2(\sqrt{\omega_1^2+m^2}-m)(\sqrt{\omega_2^2+m^2}-m) + 2F_1^2\omega_1\omega_2\vec{p}_2^{\,2}\cos\theta - 2F_1^2F_2p_{2x}\omega_1(\sqrt{\omega_2^2+m^2}-m) + 2F_1^2F_2\omega_2(p_{2x}\cos\theta + p_{2y}\sin\theta) \times (\sqrt{\omega_1^2+m^2}-m)}{\sqrt{\omega_1^2+m^2}\sqrt{\omega_2^2+m^2}\{m+\omega_1-\sqrt{\omega_1^2+m^2}\}\{m-\omega_2-\sqrt{\omega_2^2+m^2}\}} \right]. \tag{12}$$

Denoting the denominators of the three terms as $D_1^{(+)}$, $D_2^{(+)}$ and $D_3^{(+)}$ respectively, we have

$$|M^{(+)}(\mathrm{AA'})|^2$$

$$= \frac{1}{4F_1F_2}(4\pi e^2)^2 \left[\frac{1}{D_1^{(+)}} \{F_1^2F_2^2(\omega_1^2+2m^2-2m\sqrt{\omega_1^2+m^2}) + F_1^2\omega_1^2\vec{p}_2^{\,2} - 2F_1^2F_2\omega_1 p_{2x}(\sqrt{\omega_1^2+m^2}-m)\} \right.$$

$$+ \frac{1}{D_2^{(+)}} \{F_1^2F_2^2(\omega_2^2+2m^2-2m\sqrt{\omega_2^2+m^2}) + F_1^2\omega_2^2\vec{p}_2^{\,2} + 2F_1^2F_2\omega_2(p_{2x}\cos\theta + p_{2y}\sin\theta) \times (\sqrt{\omega_2^2+m^2}-m)\}$$

$$\left. + \frac{1}{D_3^{(+)}} \{2F_1^2F_2^2(\sqrt{\omega_1^2+m^2}-m)(\sqrt{\omega_2^2+m^2}-m) + 2F_1^2F_2\omega_2(\sqrt{\omega_1^2+m^2}-m) \times (p_{2x}\cos\theta + p_{2y}\sin\theta) - 2\omega_1\omega_2F_1^2\vec{p}_2^{\,2}\cos\theta - 2F_1^2F_2\omega_1p_{2x}(\sqrt{\omega_2^2+m^2}-m)\} \right]. \tag{13}$$

$$|M^{+}(BB')|^2$$

$$= \frac{1}{4F_1F_2}(4\pi e^2)^2\left[\frac{1}{D_1^{(+)}}\{F_1^2F_2^2(\omega_1^2+2m^2-2m\sqrt{\omega_1^2+m^2})\right.$$

$$+ F_1^2\vec{p}_2^{\,2}\omega_1^2 - 2F_1^2F_2\omega_1(\sqrt{\omega_1^2+m^2}-m)$$

$$\times (p_{2x}\cos 2\theta + p_{2y}\sin 2\theta)\}$$

$$+ \frac{1}{D_2^{(+)}}\{F_1^2F_2^2(\omega_2^2+2m^2-2m\sqrt{\omega_2^2+m^2}) + F_1^2\vec{p}_2^{\,2}\omega_2^2$$

$$+ 2F_1^2F_2\omega_2(\sqrt{\omega_2^2+m^2}-m)$$

$$\times (p_{2x}\cos\theta - p_{2y}\sin\theta)\}$$

$$+ \frac{1}{D_3^{(+)}}\{2F_1^2F_2^2(\sqrt{\omega_1^2+m^2}-m)(\sqrt{\omega_2^2+m^2}-m)$$

$$\times \cos 2\theta - 2F_1^2F_2\omega_1(\sqrt{\omega_2^2+m^2}-m)p_{2x}$$

$$- 2F_1^2\vec{p}_2^{\,2}\omega_1\omega_2\cos\theta + 2F_1^2F_2\omega_2$$

$$\left.\times (\sqrt{\omega_1^2+m^2}-m)(p_{2x}\cos\theta + p_{2y}\sin\theta)\}\right]. \tag{14}$$

Similarly in the case of negative energy, we have

$$|M^{-}(AB' \text{ or } BA')|^2$$

$$= \frac{(4\pi e^2)^2}{4F_1F_2}\left[\frac{F_1^2F_2^2(\omega_1^2+2m^2+2m\sqrt{\omega_1^2+m^2}) + F_1^2\omega_1^2\vec{p}_2^{\,2} - 2F_1^2F_2\omega_1p_{2x}}{\times(\sqrt{\omega_1^2+m^2}+m)}{(\omega_1^2+m^2)(2m^2+2\omega_1^2+2m\omega_1+2\sqrt{\omega_1^2+m^2}(m+\omega_1)}\right.$$

$$+ \frac{F_1^2F_2^2(\omega_2^2+2m^2+2m\sqrt{\omega_2^2+m^2}) + F_1^2\omega_2^2\vec{p}_2^{\,2} + 2F_1^2F_2\omega_2}{\times(p_{2x}\cos\theta + p_{2y}\sin\theta)(\sqrt{\omega_2^2+m^2}+m)}{(\omega_2^2+m^2)\{2m^2+2\omega_2^2-2m\omega_2+2\sqrt{\omega_2^2+m^2}(m-\omega_2)\}}$$

$$\left.+ \frac{-2F_1^2F_2^2(\sqrt{\omega_1^2+m^2}+m)(\sqrt{\omega_2^2+m^2}+m) + 2F_1^2\vec{p}_2^{\,2}\omega_1\omega_2\cos\theta}{+2F_1^2F_2\omega_1p_{2x}(\sqrt{\omega_2^2+m^2}+m) - 2F_1^2F_2\omega_2(p_{2x}\cos\theta+p_{2y}\sin\theta)}{\times(\sqrt{\omega_1^2+m^2}+m)}{\sqrt{\omega_1^2+m^2}\sqrt{\omega_2^2+m^2}\{m+\omega_1+\sqrt{\omega_1^2+m^2}\}\{m-\omega_2+\sqrt{\omega_2^2+m^2}\}}\right].$$

Denoting the denominations in (15) by $D_1^{(-)}$, $D_2^{(-)}$ and $D_3^{(-)}$ respectively, we have

$$
\begin{aligned}
&|M^{-}(AA')|^2 \\
&= \frac{(4\pi e^2)^2}{4F_1F_2}\Bigg[\frac{1}{D_1^{(-)}}\{F_1^2F_2^2(\omega_1^2+2m^2+2m\sqrt{\omega_1^2+m^2}) \\
&\qquad + F_1^2\omega_1^2\vec{p}_2^{\,2} + 2F_1^2F_2p_{2x}\omega_1(\sqrt{\omega_1^2+m^2}+m)\} \\
&\quad + \frac{1}{D_2^{(-)}}\{F_1^2F_2^2(\omega_2^2+2m^2+2m\sqrt{\omega_2^2+m^2}) + F_1^2\omega_2^2\vec{p}_2^{\,2} \\
&\qquad - 2F_1^2F_2\omega_2(p_{2x}\cos\theta + p_{2y}\sin\theta) \\
&\qquad \times(\sqrt{\omega_2^2+m^2}+m)\} \\
&\quad + \frac{1}{D_3^{(-)}}\{2F_1^2F_2^2(\sqrt{\omega_1^2+m^2}+m)(\sqrt{\omega_2^2+m^2}-m) \\
&\qquad - 2F_1^2\vec{p}_2^{\,2}\omega_1\omega_2\cos\theta + 2F_1^2F_2p_{2x}\omega_1 \\
&\qquad \times(\sqrt{\omega_2^2+m^2}+m) - 2F_1^2F_2\omega_2 \\
&\qquad \times(p_{2x}\cos\theta + p_{2y}\sin\theta)(\sqrt{\omega_1^2+m^2}+m)\}\Bigg].
\end{aligned}
\tag{16}
$$

$$
\begin{aligned}
&|M^{-}(BB')|^2 \\
&= \frac{(4\pi e^2)^2}{4F_1F_2}\Bigg[\frac{1}{D_1^{(-)}}\{F_1^2F_2^2(\omega_1^2+2m^2+2m\sqrt{\omega_1^2+m^2}) \\
&\qquad + F_1^2\omega_1^2\vec{p}_2^{\,2} + 2F_1^2F_2\omega_1 \\
&\qquad \times(p_{2x}\cos 2\theta + p_{2y}\sin 2\theta)(\sqrt{\omega_1^2+m^2}+m)\} \\
&\quad + \frac{1}{D_2^{(-)}}\{F_1^2F_2^2(\omega_2^2+2m^2+2m\sqrt{\omega_2^2+m^2}) + F_1^2\omega_2^2\vec{p}_2^{\,2} \\
&\qquad - 2F_1^2F_2\omega_2(p_{2x}\cos\theta - p_{2y}\sin\theta) \\
&\qquad \times(\sqrt{\omega_2^2+m^2}+m)\} \\
&\quad + \frac{1}{D_3^{(-)}}\{2F_1^2F_2^2(\sqrt{\omega_1^2+m^2}+m)(\sqrt{\omega_2^2+m^2}+m) \\
&\qquad \times\cos 2\theta - 2F_1^2\vec{p}_2^{\,2}\omega_1\omega_2\cos\theta + 2F_1^2F_2\omega_1 \\
&\qquad \times(\sqrt{\omega_2^2+m^2}+m)p_{2x} - 2F_1^2F_2\omega_2 \\
&\qquad \times(\sqrt{\omega_1^2+m^2}+m)(p_{2x}\cos\theta + p_{2y}\sin\theta)\}\Bigg].
\end{aligned}
\tag{17}
$$

The differential cross-sections $d\sigma$ are given by $2\pi\,|\mathbf{M}|^2 \times$ (density of states). After substituting for p_2^2, etc., in terms of ω_1 and ω_2 from the following relations we may compare the cross-sections for positive and negative intermediate energies.

$$\mathbf{F}_2 = 2m + \omega_1 - \omega_2 \quad \text{(from energy conservation)}$$

$$\vec{p}_2^{\,2} = \mathbf{E}_2^2 - m^2 = (2m + \omega_1 - \omega_2)\,(\omega_1 - \omega_2)$$

$$\mathbf{F}_1^2 = 4m^2$$

$$p_{2x} = \omega_1 - \omega_2 \cos\theta \quad \text{(from momentum conservation)}$$

$$p_{2y} = -\,\omega_2 \sin\theta.$$

Discussion

Since the expressions are rather complicated, it is difficult to compare the cross-sections for the positive and negative energy intermediate states directly. However we shall take up some special cases to get an idea of the relative contributions:

(1) Non-relativistic case, *i.e.*, $\omega_1 \ll m$ and $\omega_1 \sim \omega_2$. In the case of positive energy intermediate states

$$d\sigma^+(\mathrm{AA}') = \frac{e^4}{16m^4}\Big[(-2\omega_1)(\omega_1 - \omega_2\cos\theta)\Big(1 + \frac{\omega_1}{m}\Big)$$

$$+ (2\omega_2)(\omega_2 - \omega_1\cos\theta)\Big(1 - \frac{\omega_2}{m}\Big)$$

$$- 2\omega_2(\omega_2\cos\theta - \omega_1) - 2\omega_1^2\cos\theta\Big]$$

(neglecting terms of order ω_1^2/m^2)

$$\simeq \frac{e^4}{16m^2}\,\frac{\omega_1^2}{m^2} \sim 0. \tag{18}$$

Similarly

$$d\sigma^+(\mathrm{BB}' \text{ or } \mathrm{AB}' \text{ or } \mathrm{BA}') \sim 0.$$

Now we shall calculate the cross-section for the intermediate negative energies

$$d\sigma^{-}(\mathrm{AA}')$$

$$= \frac{e^4}{16m^2}\left[\frac{1}{4m^4\left(1+\frac{\omega_1}{m}\right)}\left\{2m\left[2m\,(4m^2+2\omega_1{}^2)\right.\right.\right.$$

$$\left.\left.\left.+\,2\omega_1\left(2m+\frac{\omega_1{}^2}{2m}\right)(\omega_1-\omega_2\cos\theta)\right]\right\}\right.$$

$$+\frac{1}{4m^4\left(1-\frac{\omega_2}{m}\right)}\left\{2m\left[2m\,(4m^2+2\omega_2{}^2)\right.\right.$$

$$\left.\left.+\,2\omega_2\left(2m+\frac{\omega_2{}^2}{2m}\right)(\omega_2-\omega_1\cos\theta)\right]\right\}$$

$$+\frac{1}{4m^4}\left\{2m\left[4m\left(2m+\frac{\omega_1{}^2}{2m}\right)\left(2m+\frac{\omega_1{}^2}{2m}\right)\right.\right.$$

$$+\,2\,(\omega_1-\omega_2\cos\theta)\,\omega_1\left(2m+\frac{\omega_1{}^2}{2m}\right)$$

$$\left.\left.+\,2\,(\omega_2-\omega_1\cos\theta)\,\omega_2\left(2m+\frac{\omega_2}{2m}\right)\right]\right\}\Bigg].$$

Neglecting $\omega_1{}^2/m^2$, we have

$$d\sigma^{-}(\mathrm{AA}') \simeq \frac{e^4}{16m^2}\left[\frac{16m^4+16m^4+32m^4}{4m^4}\right]$$

$$\simeq \frac{e^4}{m^2}. \tag{19}$$

Similarly

$$d\sigma^{-}(\mathrm{BB}') = \frac{e^4}{m^2}(\cos^2\theta) \tag{20}$$

$$d\sigma^{-}(\mathrm{AB}' \text{ or } \mathrm{BA}') = 0. \tag{21}$$

(ii) Extreme relativistic case (*a*) small angles, *i.e.*, $\omega_1 \sim \omega_2 \gg m$. The results for different polarization are tabulated below, (*b*) large angles $\omega_1 \gg m \sim \omega_2$. In this case the results are similar to the previous ones excepting that here

$$d\sigma\,(\mathrm{AB}' \text{ or } \mathrm{BA}') = d\sigma\,(\mathrm{BB}') \neq d\sigma\,(\mathrm{AA}').$$

This is to be expected since $e_1 \cdot e_2$ for $\mathrm{BB}' \sim 0$ since $\cos\theta \sim 0$.

UNIVERSITY OF MICHIGAN LIBRARIES

Differential cross-sections for Compton effect

Energy / Polarization	Non-relativistic ($\omega_1 \sim \omega_2 \ll m$)		Extreme relativistic ($\omega_1 \gg m$; $\omega_1 \sim \omega_2$) small angles	
	Positive Intermediate Energy	Negative Intermediate Energy	Positive Intermediate Energy	Negative Intermediate Energy
AA′	$\frac{e^4}{m^2}\left(\frac{\omega_1^2}{m^2}\right) \sim 0$	$\frac{e^4}{m^2}$	$\frac{e^4}{4m^2}\left(1 - \frac{m}{\omega_1} - \frac{m}{\omega_2}\right)$	$\frac{e^4}{4m^2}\left(1 + \frac{m}{\omega_1} + \frac{m}{\omega_2}\right)$
BB′	Do.	$\frac{e^4}{m^2}\cos^2\theta$	$\frac{e^4}{4m^2}\left(1 - \frac{m}{\omega_2} - \frac{m}{\omega_1}\cos 2\theta\right)$	$\frac{e^4}{4m^2}\left(1 + \frac{m}{\omega_2} + \frac{m}{\omega_1}\cos 2\theta\right)$
AB′	Do.	$\frac{e^4}{m^2}\left(\frac{\omega_1^2}{m^2}\right) \sim 0$	$\frac{e^4}{4m^2}$	$\frac{e^4}{4m^2}$
BA′	Do.	Do.	Do.	Do.

[*cf. Quantum Theory of Radiation*, by W. Heitler, (1954)].

It is interesting to note that the contributions arising from the negative energy intermediate states dominates the cross-sections in the non-relativistic limit for the electron. In fact the contribution from positive energy intermediate states is almost zero so that

$$\tfrac{1}{2}\, d\sigma^{-}(\mathrm{AA}' + \mathrm{BB}') = \tfrac{1}{2}\,\frac{e^4}{m^2}(1 + \cos^2\theta) = \tfrac{1}{2}\, d\sigma\,(\mathrm{AA}' + \mathrm{BB}')$$

$$\text{since } d\sigma^{+} = 0$$

which is the actual cross-section (*i.e.*, including both positive and negative energy intermediate states).

In the extreme relativistic case, we find that contributions arise from both positive and negative energy intermediate states. We also find that in case (*a*) $d\sigma^{+}(\mathrm{AB}') = d\sigma^{-}(\mathrm{AB}')$ though $d\sigma$ (AB′ or BA′) is zero. This can be easily seen from the fact $\mathrm{M}^{+}(\mathrm{AB}') = -\mathrm{M}^{-}(\mathrm{AB}')$ and hence $|\mathrm{M}^{+} + \mathrm{M}^{-}|^2 = 0$. Similarly for $d\sigma^{+}(\mathrm{AA}') + d\sigma^{-}(\mathrm{AA}') = e^4/2m^2$ though $d\sigma(\mathrm{AA}') = e^4/m^2$. This is again obvious since in this case $\mathrm{M}^{+}(\mathrm{AA}') \triangleq +\mathrm{M}^{-}(\mathrm{AA}')$ so that $d\sigma = |\mathrm{M}^{+} - \mathrm{M}^{-}|^2 = |2\mathrm{M}^{+}(\mathrm{AA}')|^2 = e^4/m^2$. Calculations on other electrodynamic processes will be given in a later contribution.

One of us (A. R.) wishes to express his gratitude for the hospitality and facilities extended to him by Professor Andre Mercier, Theoretical Physics Seminar, University of Bern, Switzerland, during his stay as Visiting Professor under the auspices of the Swiss Atomic Energy Commission. Miss T. K. Radha is grateful to the Atomic Energy Commission, India, for the grant of a Junior Fellowship and Miss R. Thunga to the University of Madras for the facilities afforded for work at the University.

ANALYSIS OF THE X-RAY DIFFRACTION PATTERN OF HELICAL STRUCTURES

By G. N. Ramachandran

(*Department of Physics, University of Madras, Guindy, Madras-25*)

Received August 19, 1960

Abstract

The paper deals with the theory of the diffraction pattern of helical structures having the number of units per turn (n) neither integral nor rational. The conventional treatment suffers from the defect that the repeat spacing along the axis of the helix is taken as the standard of reference, and this does not exist, being infinite, when n is irrational. The difficulty is got over in this paper by focussing attention on the 'unit height' (h = resolved component of a unit along the axis) and 'unit twist' (t = fraction of a complete rotation for one unit, $= 1/n$), which vary continuously irrespective of n being rational or irrational. Explicit formulæ are obtained in terms of their Bessel indices for the observed layer line-spacings which turn out to be very simply related to the reciprocals of the unit height and the pitch of the helix. A technique of analysing the observed diffraction pattern for the elements of the helical structure is also given, with examples. The case of a coiled-coil is seen to have the same general features as the simple coil, the layer line-spacing being now related to two pitches, namely, those of the major and the minor helices, and the unit height. The relationship of the diffraction pattern of a helix in its uncoiled and its coiled-coil form is also found to be rather simple, being similar to the multiplet splitting produced by a magnetic field in spectral lines.

1. Theory for a Simple Helix with a Non-integral Screw Axis

It is well known that the characteristic feature of the X-ray diffraction pattern of a fibre containing helical chains, with the number of links (units) per turn, n, non-integral, is the occurrence of strong layer lines whose layer-spacings are not all in the ratio of 1 : 2 : 3, etc., as is found in the rotating crystal diagram of an ordinary crystal. An explanation of this was given in terms of the Fourier transform of a helical structure by Cochran, Crick and Vand (1952). Taking in particular the case of M point atoms arranged at regular intervals in N turns of a helix of radius r and pitch P, so that the

repeat spacing along the axis is $c = NP$, the intensity distribution in reciprocal (Fourier) space (R, ψ, Z) on the layer line l with $Z = l/c$ essentially depends on the value of the Bessel function $J_q(2\pi Rr)$, where q is an integer which satisfies the equation

$$Nq + Mm = l \qquad (q,\ m,\ l \text{ integers}). \tag{1}$$

Now denote the projected distance between two successive atoms along the axis of the helix by $h\,(= c/M)$, which may be called the 'unit height', and the fraction of a full rotation corresponding to one such unit by $t\,(= N/M)$, which may similarly be called the 'unit twist'. Clearly the unit twist is the reciprocal of the number of units per turn, *i.e.*,

$$\boxed{t = \frac{1}{n}.} \tag{2}$$

Since only $J_0(x)$ has a finite value for $x = 0$, all other $J_q(x)$ being zero for $x = 0$, and since the first maximum of $J_q(x)$ occurs for larger and larger values of x and is relatively lesser in height as q increases, it follows that the prominent layer lines are those for which q is a small integer and of these only those with $q = 0$ contain a meridional reflection. Thus, restricting ourselves to layer lines with spacings between c and $c/M = h$, *i.e.*, $l = 1$ to M, the principal layer lines are seen to be as below*:

For $q = 0$,	$l = M$;	$Z = M/c$;
For $q = 1$,	$l = N,\ M - N$;	$Z = N/c,\ (M - N)/c$;
For $q = 2$,	$l = 2N,\ M - 2N$;	$Z = 2N/c,\ (M - 2N)/c$.

Now, suppose that the helix undergoes a small deformation, so that the unit twist t, which was equal to N/M, increases very slightly (say). It is obvious that the repeat spacing c would completely change, *e.g.*, taking the α-helix with $h = 1{\cdot}5$ A, $n = 3{\cdot}6$, which corresponds to $N = 5$, $M = 18$, $c = 27$ A, if n increases to $3{\cdot}625$, then $N = 8$, $M = 29$, $c = 43{\cdot}5$ A, while if n increases to $3{\cdot}61$, then $N = 100$, $M = 361$, $c = 541{\cdot}5$ A. Thus, the repeat spacing c undergoes wild fluctuations as the number of units per turn (n) or t is changed even by a minute amount—actually $c \to \infty$ if n is irrational. However, it stands to reason from physical grounds that the diffraction pattern would only undergo an infinitesimal change for such an infinitesimal change in n or t. Actually, that this is so can be verified by

* These conclusions continue to hold even when there are a number of atoms in the repeating unit, provided they all follow the same helical pattern, as is the case in a helical structure, which is fully specified by the two parameters h and t (or n).

fully working out the pattern according to the above theory for various rational approximations to a given number. This point has been recognised by Cochran *et al.* (1952), but they have not considered the general case. It would, therefore, be worthwhile reformulating the theory in such a manner that no such rational approximation is needed. As will be shown below, it turns out that what is relevant to the specification of a helical structure are the parameters unit height (h) and the unit twist (t). The repeat spacing c need not enter the picture at all in the formulation. It is obvious that, from the stereochemical point of view also, the only data that are specified for a helical chain is the relationship between one unit and the next, which is precisely the same between that and the next and so on. The repeat spacing c is never specified as such.†

Thus, since c is unspecified, the only reciprocal spacing which can be used to describe the pattern is the reciprocal of the unit height h, *i.e.*, $1/h = Z_0$ (say). This is in fact the spacing of the meridional reflection. Therefore, let $Z = \eta Z_0$, instead of l. $(1/c)$ as before. Then, in Eqn. (1) $l = \eta c/h = \eta M$, so that we have

$$Nq + Mm = \eta M,$$

or dividing by M throughout and remembering that $N/M = t$, we have

$$tq + m = \eta, \qquad Z = \frac{\eta}{h} = \eta Z_0. \tag{3}$$

The layer lines are now given by the number η, which is not an integer (and which is not even necessarily a rational number). The prominent layers correspond to $q = 0, 1, 2, \ldots\ldots$ in decreasing order of prominence. Consequently, it would be more useful to use the Bessel index q to denote the layer lines in the diffraction pattern of a helix, and the corresponding $\eta_q = (tq + m)$ gives its location.

In order to get a clearer picture, let us restrict ourselves to layers with $|Z| < 1/h$, *i.e.*, those occurring within the first meridional reflection. Taking $n = 3{\cdot}6$ as for the α-helix, $t = 0{\cdot}278$ and the layers with Bessel indices $|q| = 0, 1, 2, 3, 4$ occur at $Z = Z_0$, $Z = 0{\cdot}278Z_0$ and $0{\cdot}722Z_0$, $Z = 0{\cdot}556$ and $0{\cdot}444Z_0$, $Z = 0{\cdot}834$ and $0{\cdot}166Z_0$, $Z = 0{\cdot}112$ and $0{\cdot}888Z_0$.

† It has been possible to work out specific formulæ, which give (*a*) the orientation of the helical axis, (*b*) the unit height and (*c*) the unit twist (t) when the stereochemical relations between successive units are given, but this will be reported separately.

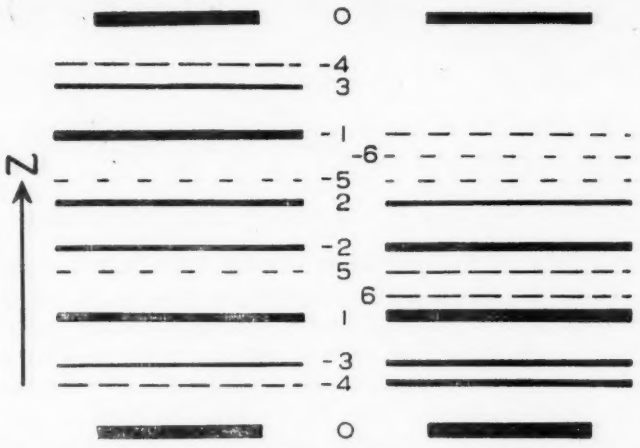

FIG. 1. (*a*) Schematic diagram, showing layer lines of a simple helix with $n = 3{\cdot}6$. The thickness of each layer roughly represents its intensity. (*b*) Relative intensities of the layers actually observed with poly-L-alanine. Note the occurrence of layers even with large q (up to 6) at low angles (small Z), but the relative absence of layers at larger values of Z.

These are schematically shown in Fig. 1 and the general formula may be written in the form:

$$Z_q = [[qt]]\, Z_0 \quad \text{and} \quad Z_q' = (1 - [[qt]])\, Z_0, \tag{4}$$

where $[[x]]$ stands for the fractional part of x. Those with $q = 0$ are meridional, while the others are non-meridional. In terms of the X-ray crystallographic $\zeta = \lambda Z$, the ζ-values of the prominent layer lines can be deduced from Eqn. (4) to occur at

$$\zeta = [[qt]]\frac{\lambda}{h} \quad \text{and} \quad \zeta = (1 - [[qt]])\frac{\lambda}{h}. \tag{5}$$

It will be noticed that these very simple formulæ contain no reference at all to the repeat spacing c, but require only the specification of h, the projected height of one unit along the axis of the helix and n, the number of units per turn. The formulæ are equally valid when n is integral or is the ratio of (simple) integers. Since, in the limit when n tends to an irrational number, there is no quantity in the formulæ which fluctuates indefinitely, the formulæ are also true in the limit when n is irrational. Thus, they can be taken to be valid quite generally. Then, the intensity distribution in reciprocal space on a layer of Bessel index q is given by the formula of Cochran *et al.*, *viz.*,

$$F(R, \psi, Z) = \sum_j \sum_q f_j J_q(2\pi R r_j) \exp i \left[q\left(-\psi + \phi_j + \frac{\pi}{2}\right) + 2\pi Z z_j \right] \quad (6)$$

where (r_j, ϕ_j, z_j) is the position of a j-th type atom and f_j is its scattering factor, and Z is given by Eqn. (3).

2. Analysis of Layer Lines by the New Formula

The new form of the diffraction formula for a helical structure given by Eqn. (3) will be found to be very useful in practice as will be evident from some examples to be given below. Thus, in interpreting a helix diffraction pattern, the first thing to look for should be the truly meridional reflections. Owing to disorder, some non-meridional reflections would occur as arcs bridging the meridian, but these can in many cases be resolved by taking inclined fibre photographs. So also, the truly meridional reflection can be brought out by such a photograph, as in the case of the 1·5 A of the alpha helix. Having thus obtained h and hence ζ_0 (or Z_0), the next step should be to look for the other prominent layer lines with $\zeta < \zeta_0$. If two such can be found, say ζ, ζ' such that

$$\zeta + \zeta' = \zeta_0, \quad (7)$$

then it is clear from Eqn. (5) that

$$\zeta, \zeta' = (qt)\,\zeta \quad \text{and} \quad (1 - qt)\,\zeta_0, \quad (8)$$

most probably with $q = 1$, so that ζ/ζ_0 gives at once the unit twist t, and n, the number of units per turn of the helix. Sometimes q may not be equal to one, but 2 for the most prominent layer lines owing to the fact that the Fourier transform of the unit itself is weak near the meridian corresponding to the layers with $q = 1$. In any case, further confirmation of the assignment can be obtained by comparing the ζ-values of the other observed layer lines with the values calculated from Eqn. (5).

Thus, it is seen that the analysis of the X-ray diffraction pattern of a helix for its elements h and t (or n) is quite straightforward, so long as the layer lines are clear and the meridional and non-meridional reflections can be clearly distinguished. We shall illustrate the procedure with reference to the data on the α-form of poly-γ-methyl-L-glutamate (Bamford *et al.*, 1956). The mean values of ζ for the observed layer lines are 0·109, 0·173, 0·2865, 0·461 and 1·028, the last of which is meridional. The strongest layer is the one with $\zeta = 0{\cdot}2865$,

Obviously $\zeta_0 = 1{\cdot}028$, giving $h = 1{\cdot}50$ A. A more accurate value of $\zeta_0 = 1{\cdot}034$ may be deduced from the later data of Brown and Trotter (1956) which is also in agreement with the measurement $h = 1{\cdot}491$ A of Yakel (1953). No two of the ζ's satisfy an equation of the form (7). However,

$$2 \times 0{\cdot}2865 + 0{\cdot}461 = 1{\cdot}034$$

and

$$3 \times 0{\cdot}2865 + 0{\cdot}173 = 1{\cdot}0325$$

and the sum in either case is close to $\zeta_0 = 1{\cdot}034$. From the general theory, these equations are consistent with the assignment

$$\begin{aligned} 0{\cdot}2865 &= t\zeta_0 && (q = 1) \\ 0{\cdot}461 &= (1 - 2t)\,\zeta_0 && (q = -2) \\ 0{\cdot}173 &= (1 - 3t)\,\zeta_0 && (q = -3) \end{aligned}$$

The mean value of $n(= 1/t)$ obtained from these assignments is $3{\cdot}58$. This value leads to $\zeta_4 = (4t - 1)\,\zeta_0 = 0{\cdot}106$, which is close to the observed value of $0{\cdot}109$.

Thus, our analysis shows that the observed pattern is consistent with a structure with $h = 1{\cdot}491$ A and $n = 3{\cdot}58$. Actually Bamford *et al.* have tried to index their observations on the basis of a cell with M = 29, N = 8 giving $n = 3{\cdot}625$ and M = 69, N = 19, *i.e.*, $n = 3{\cdot}632$ in addition to the simple $n = 3{\cdot}6$ helix with M = 18, N = 5. If $\zeta_0 = 1{\cdot}028$ is used, the mean value of n obtained is $3{\cdot}61$ (variation $3{\cdot}58$ to $3{\cdot}64$), which is close to the rational approximation attempted. These facts suggest that the rational approximations are not particularly relevant, unless they are dictated by some special considerations such as symmetry.

A similar analysis may be made of the pattern of α-poly-L-alanine (Brown and Trotter, 1956; Bamford *et al.*, 1956). Brown and Trotter have given a table of observed ζ's of the various layer lines conveniently as reciprocal spacings Z in A^{-1}. We shall designate the layers by A, B, C....K whose Z-values are listed in Table I. The last one K with $Z_K = Z_0 = 0{\cdot}668_6$ is the only meridional reflection, giving $h = 1{\cdot}495$ A.

Of these, $Z_C + Z_J = 0{\cdot}665 \simeq 0{\cdot}668_6$ and C is a prominent layer line, so that we may identify these with $q = 1$, giving $Z_C = tZ_0$ and $Z_J = (1 - t)\,Z_0$. Now, from Eqn. (3) it follows that

$$\frac{Z}{Z_0} = \eta = m \pm qt. \tag{9}$$

TABLE I

List of observed layer lines and their indexing by Bessel indices q *for poly-L-alanine. Note that layer lines with* q = 3, 4 *at* 0·555 *and* 0·597 *are absent while those with* q = 5, 6 *actually occur*

Layer line	Z	$\|q\|$	Z/Z_0 (from theory)	$Z_1 = tZ_0$ (from obsn.)
A	0·0713	4	$4t-1$	0·1850
B	0·114	3	$1-3t$	0·1849
C	0·185	1	t	0·1850
D	0·233	6	$2-6t$	0·1840
E	0·257	5	$5t-1$	0·1851
F	0·298	2	$1-2t$	0·1858
G	0·367	2	$2t$	0·1835
H	0·411	5	$2-5t$	0·1852
I	0·433	6	$6t-1$	0·1836
J	0·480	1	$1-t$	0·1886*
K	0·6686	0	1	..
			Mean ..	0·185 ± 0·001

* Omitted in obtaining the average and standard error.

From this, it is obvious that a number of observed Z-values must differ by multiples of $Z_1 (= tZ_0)$. It will be seen that this is in fact true. Thus,

$$Z_E - Z_A = 0{\cdot}185$$
$$Z_F - Z_B = 0{\cdot}184$$
$$Z_G - Z_C = 0{\cdot}182$$
$$Z_H - Z_D = 0{\cdot}178$$
$$Z_I - Z_E = 0{\cdot}176$$
$$Z_J - Z_F = 0{\cdot}182$$
$$Z_K - Z_J = 0{\cdot}188_6$$

This clearly establishes that our identification of $Z_1 = 0{\cdot}185$ by $q = 1$ is correct. A further confirmation of this comes from the fact that $Z_F + Z_C = 0{\cdot}665 \simeq Z_K$ and the relation $Z_F \simeq 2Z_C$ holds. The indexing of all the observed layers is, thereafter, straightforward. The values of q are given in the third column and the value of Z/Z_0 from theory in the fourth column.

Using the data from the fourth column, the value of $Z_1 (= tZ_0)$ is deduced from each of the measurements and they are given in column 5. It will be seen that all of them are very nearly a constant except the one deduced from Z_J which has a larger error. This layer is very weak in the diagram and so this value may be omitted in finding the mean which comes out to be $0{\cdot}185 \pm 0{\cdot}001$, where the $\pm$ gives the standard error. Taking the value of Z_0 to have a relative error of $\pm 0{\cdot}2\%$, as given by Brown and Trotter, we find that

$$n = 3{\cdot}615 \pm 0{\cdot}02.$$

It is interesting that the mean value is identical with that assumed by Brown and Trotter, namely, $47/13 = 3{\cdot}615$. However, their quoted probable error $\pm 0{\cdot}003$ is far too small. It is not clear how they have deduced their probable error, but their own data giving $\zeta_{obs.}$ and $\zeta_{cal.}$ in their Table I (their ζ is our Z) show a percentage deviation of the order of 1% (*e.g.*, 0·233–0·228, 0·433–0·441, 0·480–0·484, etc.) which would be more in accord with our standard error (0·6%) than theirs (<0·1%). This shows that the experimental data cannot prove that a chosen rational approximation is the correct one.

Thus, it will be seen that the analysis of the diffraction pattern of a simple helix can be made into a simple routine. This is so even if the truly meridional reflection does not record, for Z_0 can be deduced from the fact that pairs of Z-values will have their sums equal. In the present case, we have several such, *e.g.*,

$$\begin{aligned} Z_J + Z_C &= 0{\cdot}665 \\ Z_I + Z_D &= 0{\cdot}666 \\ Z_H + Z_E &= 0{\cdot}668 \\ Z_G + Z_F &= 0{\cdot}665 \\ \text{Mean} &= 0{\cdot}666 \end{aligned}$$

It will be noticed that the mean is nearly equal to the directly measured value of Z_0 (namely 0·6686) which is highly satisfactory. Modifications of these methods could, of course, be worked out to suit particular cases.

So also, it is seen that, in the ordinary way, it is not possible to prove that there is a definite repeat spacing c in which the helix makes an integral number of turns. Actually, in such structures, which are not stablilised by rigid bonds connecting one helix with another, small variations are likely to occur, and the interesting fact that has come out of the present study is that such variations only insignificantly affect the diffraction patterns. The layer lines may be slightly shifted about (not all in the same direction), but the strong ones would continue to be strong and the weak ones weak.

3. THEORY FOR A COILED-COIL

In the above discussion, we have been dealing only with simple helices. When there is a further coiling of these, leading to superhelical configurations, the nature of the diffraction pattern changes somewhat. In order to get the picture clearly, we shall write the formula of Crick (1953) connecting the various Bessel functions orders in a form more akin to our equations (1) and (8). His equation is, with a small change in notation (N_1' instead of N_1),

$$N_0 p + (N_1' - N_0)\, q + N_1' s + (N_1' + N_0)\, d + Mm = l,$$

with p, q, s, d, m, l integers (10)

for a layer line with $Z = l/c$, c being the repeat spacing which contains M units, N_0 turns of the major helix and N_1' turns of the minor helix. Let $n_0 = M/N_0$ be the number of units per turn of major helix, $n_1' = M/N_1'$, the number of units per turn of the minor helix in a rotating frame of reference following the major helix. As in the case of the simple helix, write $Z = \eta \cdot (1/h)$, so that $l = \eta M$ and let $t_0 = 1/n_0$, $t_1' = 1/n_1'$. Then Eqn. (10) becomes

$$t_0 p + (t_1' - t_0)\, q + t_1' s + (t_1' + t_0)\, d + m = \eta \qquad (11\,a)$$

$$Z = \eta Z_0,\ Z_0 = \frac{1}{h}. \qquad (11\,b)$$

Thus, the repeat spacing c has disappeared and the layer is now specified by the number η (not necessarily even rational) which corresponds to the Bessel indices (p, q, s, d). The intensity distribution in this layer continues to be given by Crick's Eqn. (13) for a coiled-coil with one atom per unit having unit scattering factor (*see* his paper for details of notation):

$$F(R, \psi, Z) = \sum_p \sum_q \sum_s \sum_d J_p(2\pi R r_0)\, J_q(2\pi R \bar{r}_1) \,.\, J_s(2\pi Z r_1 \sin\alpha)\, J_d(2\pi R \Delta)$$
$$\times \exp i \left[p\left(\psi - \phi_0 + \frac{\pi}{2}\right) + q\left(-\psi + \phi_1 + \frac{\pi}{2}\right) \right.$$
$$\left. + s(-\phi_1 + \pi) + d\left(\psi + \phi_1 + \frac{\pi}{2}\right) - m\phi_M + 2\pi Z z_0 \right]. \quad (12)$$

The most prominent layer lines correspond to small values of p and q. The index $s = 0$ for all layer lines with $Z \ll Z_0$ but $s = 1$ may occur for $Z \sim Z_0$. The index d must be put zero in most cases.

Before working out the consequences of Eqn. (11) under these conditions, it is worthwhile examining the relation between the transform of a coiled-coil and of the simple coil from which it has been obtained. Now in Crick's paper, N_1' is the number of rotations made by the minor helix in a rotating frame which rotates along with the major helix. (Crick calls this 'the number of rotations made by the minor helix *in its own frame of reference*', which appears to be not a happy wording, although its connotation is quite clear in his paper.) Now consider the number of turns N_1 made by the minor helix in space when the major helix makes N_0 turns. Under the conditions adopted in Crick's paper (left-handed minor helix, right-handed major helix, *i.e.*, the senses are opposite), it will make a smaller number of turns than N_1', actually $N_1 = N_1' - N_0$. The significance of N_1 is best visualised by considering the case when the radius of the major helix shrinks to zero. There is no coiled-coiling in such a case and N_1 is then the number of turns made by the minor helix in the repeat c. The number N_1 thus specifies the undistorted minor helix (and not N_1') and consequently it is used in all the formulæ derived below.

Thus, let N_1 be the number of turns of the minor helix in the repeat c. The associated number $n_1 = M/N_1$ is the number of units per turn of the minor helix and its reciprocal $t_1 = 1/n_1$ is its unit twist. In terms of these, Eqns. (10) and (11) become

$$N_0 p + N_1 q + (N_1 + N_0)\, s + (N_1 + 2N_0)\, d + Mm = l \quad (13)$$

$$t_0 p + t_1 q + (t_1 + t_0)\, s + m = \eta \quad (14)$$

where d is put zero in Eqn. (14). Eqn. (12) continues to be valid with this notation also.

We shall now consider the consequences of these equations,

(*a*) $s = 0$,

As already mentioned, $J_s(2\pi Zr_1 \sin\alpha)$ does not have appreciable values for small Z, except for $s = 0$. In such a case, we get

$$t_0 p + t_1 q + m = \eta, \quad Z = \eta Z_0 \tag{15}$$

which may be compared with Eqn. (3) where $t = t_1$. In general t_0, the unit twist of the major helix, will be much less than t_1 that of the minor helix so that $t_0 p \ll t_1 q$. Thus the effect of coiled-coiling is to split up each of the layers given by the simple helix into a series of closely spaced layers, becoming weaker on either side of the original one for the simple coil. This follows from the fact that $J_p(2\pi Rr_0)$ and $J_q(2\pi R\bar{r}_1)$ occur multiplied together. The situation is shown schematically in Fig. 2 for two cases (*a*) $t_0 \ll t_1$ and (*b*) $t_0 \sim t_1$. There is a close analogy to the multiplet structure of spectral lines, which might have struck the reader even in the case of the simple helix diffraction pattern (*e.g.*, the occurrence of constant differences, constant sums, etc.). The multiplets (p different) may be close together or well separated depending on t_0 being small compared to t_1 or not.

Thus, it is seen that there is no meaning in asking whether supercoiling exists or not, but only whether it is appreciable or not, for when the pitch of the major helix is very large, we would only find a slight broadening of the observed layer lines.

(*b*) $s \neq 0$.

Since $(t_0 p + t_1 q)$ contains also all the values occurring in the sum $t_0 p + t_1 q + (t_0 + t_1)s + (t_0 + 2t_1)d$, no layer lines can occur at positions other than those given by Eqn. (15) and sketched in Fig. 2. On the other hand, the functions J_s and perhaps also J_d with $s, d \neq 0$ may also contribute to some of the reflections. Thus, their intensity might be quite prominent.

Important examples of this type are the possible layer lines near $Z_0(\eta \simeq 1)$ for which $J_1(2\pi Zr_1 \sin\alpha)$ with $s = 1$ has an appreciable value. In such a case, for $q = 0$, $p = -1$, -2, etc., there occur layer lines at

$$Z = Z_0, \; Z_0(1 - t_0), \; Z_0(1 - 2t_0), \; \text{etc.},$$

i.e., a series of layer lines with constant differences corresponding to $t_0 Z_0$. Such layer lines cannot occur for a simple helix, and since $q = 0$, they will occur very near the meridian.

In fact the simplest way of finding the value of t_0 seems to be to look for such layers close to $Z = 0$ and $Z = Z_0$.

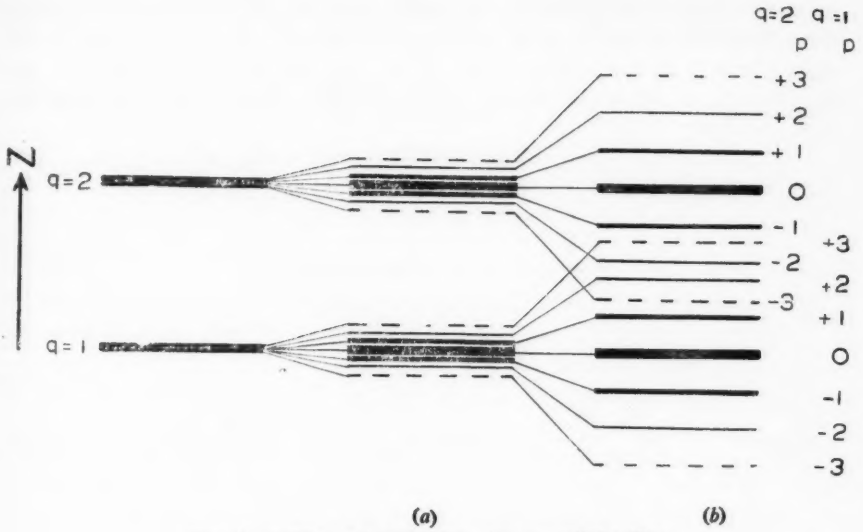

FIG. 2. Splitting of layer lines due to coiled-coiling.

Thus, the main point of interest is that the diffraction pattern of a coiled-coil is not frightfully complicated, in spite of the fact that Eqn. (13) giving the Bessel indices contains four different parameters. In terms of our analysis, it is seen that the layer lines have only two types of periodicities:

(*a*) $t_0 Z_0$ due to the major helix

(*b*) $t_1 Z_0$ due to the minor helix

and the actual layer line spacings are given by Eqn. (15). Consequently, if the Z-values of the layer lines are accurately measured, they must be fitted to a formula of the type

$$Z = mZ_0 + p\Xi_0 + q\Xi_1 \quad (m,\ p,\ q \text{ integers}). \tag{16}$$

Of these, the layer line with $Z = Z_0$ has intensity on the meridian, those with $Z = Z_0 \pm p\Xi_0$ have intensity close to the meridian, while the others are definitely non-meridional. Having found Z_0, Ξ_0, Ξ_1, the elements of the coiled-coil are given by

$$h = \frac{1}{Z_0}, \quad t_0 = \frac{\Xi_0}{Z_0}, \quad t_1 = \frac{\Xi_1}{Z_0}. \tag{17}$$

In view of the above results, the nature of the diffraction pattern when there is a still further coiling is easy to work out. If n is the number of units per turn in the primitive coil, n' the corresponding number for the first superhelix and n'' for the second superhelix, then the layer lines which occur are at

$$Z = \eta Z_0 \tag{18 a}$$

where

$$\eta = t''u + t'p + tq + m \ (u, p, q, m \text{ integers}) \tag{18 b}$$

and

$$t = \frac{1}{n}, \quad t' = \frac{1}{n'}, \quad t'' = \frac{1}{n''} \tag{18 c}$$

analogous to Eqn. (15). Obviously, layers with u, p, q small will be the strong ones.

4. CONCLUSION

If one examines Eqns. (3), (15) and (19) respectively for a simple helix, a coiled-coil and a coiled-coiled-coil, it will be seen that they are all of the same essential form. The strong layer lines occur at Z-values which, when expressed as a fraction η of the fundamental reciprocal spacing $Z_0 = 1/h$, have a direct relation to the unit twists of the various helices. In the simple helix, the various η's are just multiples of the unit twist (*cf.* $\eta = tq + m$, with q, m integral). With further coiling, the periodicities of the other (major) helices show up as a fine structure modulating the diffraction pattern of the simple helix.

In other words, if the observed data are plotted on the η-scale, *i.e.*, dividing the observed reciprocal spacing of the unit height, then they would exhibit one, two or more periodicities, according to the number of coilings in the strucure. The problem is then only of finding this periodicity, taking into account the fact that some of the layers may not be observed because they are too weak. In general, the strongest layer line ($Z = Z_1$) corresponds to $q = 1$ and its spacing $P = 1/Z_1$ would then be the pitch of the helix (as already stated). The spacing of the meridional reflection $h = (1/Z_0)$ gives the unit height. The ratio of the two gives at once the unit twist $t\,(= h/P)$ or the number of units per turn $n\,(= P/h)$. Although these are inherent in the earlier formulæ, they are again explicitly given here to emphasize the simple relationship between the diffraction pattern and

the elements of the helix. In fact, if the two halves of Eqn. (3) are combined, we get

$$Z = mZ_0 + q(tZ_0) = m \cdot \frac{1}{h} + q \cdot \frac{1}{P} \tag{20}$$

where m and q are integrals. Thus, the prominent layer lines in the diffraction pattern occur at positions related to the reciprocal of the unit height and of the pitch. The so-called repeat spacing along the helical axis is nowhere in the picture.

The extension to the case of the coiled-coil is obvious and combining the two halves of Eqn. (15), we get

$$Z = mZ_0 + p(t_0Z_0) + q(t_1Z_0) = m \cdot \frac{1}{h} + p \cdot \frac{1}{P_0} + q \cdot \frac{1}{P_1} \tag{21}$$

where P_0, P_1 are now the pitches of the major and the minor helices. The positions of the layer lines now depend only on the reciprocal of the unit height and the reciprocal of the pitches of the major and minor helices.

The great advantage of the new formalism is that one is able to get out of the restrictions imposed by rational relations. It is obvious that the degree of coiling or supercoiling, when it exists, is determined only by interatomic valence forces and that, so long as no rigid ordering imposed by a crystal lattice exists, it is not limited by any integral or rational conditions. This view-point has greatly helped in solving the helical structure of feather keratin (to be published elsewhere). So also even in the collagen structure which has been considered in the past by the author himself to have exactly 10 residues in 3 turns, a more careful study seems to indicate that no such *exact* relationship exists, although actually the number of residues per turn observed is close to it (also to be published elsewhere).

This turning away from the law of rational numbers was started by Pauling and co-workers (1951) when they put forward the idea of non-integral helices, *i.e.*, that helices with n not equal to an integer can occur in protein structures. It now appears that there is nothing sacrosanct in the use of rational numbers and that any helix can occur in a fibre structure and that it need not have even a rational number of residues per turn.

It must be stated however that if such helices form a crystal lattice with rigid interhelical bonds which are strictly repeated by translational symmetry, then the rules of classical crystallography do hold and no values other than $n = 1, 2, 3, 4$ or 6 can occur in such a structure.

5. REFERENCES

1. Bamford, C. H., Elliott, A. and Hanby, W. E. — *Synthetic Polypeptides*, New York, Academic Press Inc., 1956.
2. Brown, L. and Trotter, I. F. — *Trans. Faraday Soc.*, 1956, **52**, 537.
3. Cochran, W., Crick, F. H. C. and Vand, V. — *Acta. Cryst.*, 1952, **5**, 581.
4. Crick, F. H. C. .. — *Ibid.*, 1953, **6**, 685.
5. Pauling, L., Corey, R. B. and Branson, H. R. — *Proc. Nat. Acad. Sci. Wash.*, 1951, **37**, 205.
6. Pauling, L. and Corey, R.B. — *Ibid.*, 1951, **37**, 241.
7. Yakel, H. L. .. — *Acta Cryst.*, 1953, **6**, 724.

977–60 Printed at the Bangalore Press, Bangalore City, by T. K. Balakrishnan, Superintendent. and Published by The Indian Academy of Sciences, Bangalore.

NOTICE TO AUTHORS

Scientific papers intended for publication in the *Proceedings of the Indian Academy of Sciences* can be accepted only when they are communicated by a Fellow of the Academy whose duty shall be to satisfy himself that such communications are fit to be read at the Meeting of the Academy and published in its *Proceedings*.

Papers should not ordinarily exceed fifty pages of foolscap. MSS. should be either typewritten or written in legible hand on one side of the paper. All papers should be carefully revised by the authors and should be absolutely in final form for printing. Position for text-figures should be indicated. Each paper shall conclude with a critical summary not exceeding 350 words.

Drawings, diagrams or other illustrations should be made on larger scale (preferably) twice the size than the ones in which they are intended to appear. They should be done in Indian ink on bristol board with lettering in pencil. Scale of magnification of camera lucida tracings should be indicated by the side of drawings. In certain special cases arrangements will also be made for monochrome lithographic and other colour plates. Reduction of illustrations desired should be indicated in pencil. Appropriate legends should accompany all drawings. Names of authors are to be marked in pencil on the left-hand corner of drawing sheets. Photomicrographs should be securely mounted with colourless paste.

All tables, quotations and footnotes which will be set hereafter (beginning from Vol. I, No. 2) in types smaller than the text, should be typewritten on separate sheets and placed with the text in proper sequence. Footnotes should be numbered in Arabic numerals.

References to literature in the text should be given, whenever possible, in chronological order, only the names of authors and years of publication, in brackets, being given. They should be cited in full after the summary, the authors' names following in alphabetical order. Thus,

Name or Names of author; Name of Journal (abbreviation) with a single underline; Year of publication; Number of Volume with a double underline, and lastly page. The following would be a useful illustration:—

Bergmann and Stather . . . . . Z. Physiol. Chem., 1926, 152, 189.

Two copies of slip-proof and wherever possible, a page proof for final revision will be sent to authors. All corrections are best made on the slip-proof which should be transmitted to the Office of the Academy. All proof corrections involve heavy expenses which would be negligible if the papers are carefully revised by the authors before submission.

Fifty free reprints including plates and with cover will be supplied for each paper. Additional copies can be supplied at cost on previous intimation.

Blocks appearing in the *Proceedings* will be available for purchase by their respective authors. Orders for the same should be sent along with the corrected proofs and in any case not later than one month after the date of publication of the paper. The price charged would be 25% of the actual cost of the blocks *plus* freight and despatching charges. If the blocks are reproduced in other journals or publications, due acknowledgment should be made in them to the *Proceedings*.

The original drawings and plates of blocks appearing in the *Proceedings* will be returned to such of the authors as may require them provided the cost of despatching such originals is borne by them.

CONTENTS

PAGE

The Luminescence Spectra of Diamond . . . . . A. Jayaraman 189

Conductometric Determination of a Few Physico-Chemical Constants of Murexide . . . . . N. A. Ramaiah and R. K. Chaturvedi 197

Deviations from Parallelism and Equidistance in Finsler Space . . . . . Nirmala Prakash and Ram Behari 209

On the Decomposition of the Feynman Propagator . . . . . Alladi Ramakrishnan, T. K. Radha and R. Thunga 228

Analysis of the X-Ray Diffraction Pattern of Helical Structures . . . . . G. N. Ramachandran 240